

Organometallic Reactivity on a Calix[4]arene Oxo Surface. Synthesis and Rearrangement of Zr–C Functionalities Anchored to a Calix[4]arene Moiety

Luca Giannini,[†] Alessandro Caselli,[†] Euro Solari,[†] Carlo Floriani,^{*,†}
 Angiola Chiesi-Villa,[‡] Corrado Rizzoli,[‡] Nazzareno Re,[§] and Antonio Sgamellotti[§]

Contribution from the Institut de Chimie Minérale et Analytique, BCH, Université de Lausanne, CH-1015 Lausanne, Switzerland, Dipartimento di Chimica, Università di Parma, I-43100 Parma, Italy, and Dipartimento di Chimica, Università di Perugia, I-06100 Perugia, Italy

Received March 13, 1997[⊗]

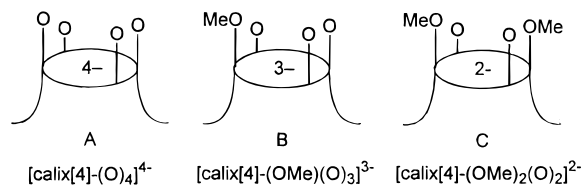
Abstract: This report concerns the formation and the main properties of Zr–C functionalities supported by the O₄ matrix of either the monoalkylated (trianionic) or dialkylated (dianionic) forms of [*p*-Bu^t-calix[4]arene] (**1**). The synthesis of the starting materials [*p*-Bu^t-calix[4]-(OMe)₂(O)₂ZrCl₂] (**4**) and [μ-*p*-Bu^t-calix[4]-(OMe)(O)₃]₂Zr₂Cl₂] (**10**) has been performed *via* the lithiation of the corresponding protic forms, [*p*-Bu^t-calix[4]-(OMe)₂(OH)₂] (**2**) and [*p*-Bu^t-calix[4]-(OMe)(OH)₃] (**8**), followed by reaction with ZrCl₄·(thf)₂. Complex **4** undergoes a facile base-induced (base = Et₃N, Py) demethylation, leading to the monomethoxy derivative [*p*-Bu^t-calix[4]-(OMe)(O)₃ZrCl₂][−][MeNEt₃]⁺ (**5**) and ionization of the Zr–Cl bond to give [*p*-Bu^t-calix[4]-(OMe)₂(O)₂Zr(OTf)₂] (**6**). The alkylation of **4** led to the corresponding dialkylaryl derivatives [*p*-Bu^t-calix[4]-(OMe)₂(O)₂ZrR₂] (R = Me, **12**; R = CH₂Ph, **13**; R = CH₂-SiMe₃, **14**; R = *p*-MeC₆H₄, **15**). They undergo a base-induced demethylation and dealkylation illustrated by the obtention of [*p*-Bu^t-calix[4]-(OMe)(O)₃Zr(CH₂Ph)(Py)] (**18**), while the thermal decomposition gave a particularly interesting result in the case of **15**, with the formation of the corresponding η²-benzynes, [*p*-Bu^t-calix[4]-(OMe)₂(O)₂-Zr(η²-MeC₆H₃)] (**16**). Cationic alkyl derivatives of zirconium have been obtained, in the case of **13**, using the monoelectronic oxidizing agent [Cp₂Fe]⁺ or a strong Lewis acid such as [B(C₆F₅)₃], [*p*-Bu^t-calix[4]-(OMe)₂(O)₂-Zr(CH₂Ph)]⁺BPh₄[−] (**19**); [*p*-Bu^t-calix[4]-(OMe)₂(O)₂Zr(CH₂Ph)(thf)]⁺BPh₄[−] (**20**); and [*p*-Bu^t-calix[4]-(OMe)₂(O)₂-Zr(CH₂Ph)]⁺[B(C₆F₅)₃(CH₂Ph)][−] (**21**). The cationic alkyl derivatives undergo easy demethylation by pyridine to give **18**. The alkylation of **10** with LiPh led to a dimeric dimetallic aryl compound, [μ-*p*-Bu^t-calix[4]-(OMe)(O)₃]₂-Zr₂Ph₂] (**22**), where the calix[4]arene unit bridges two metal atoms and the methoxy groups are only weakly bound to the metal. The spectator methoxy group binds strongly to the metal in the monomeric η²-iminoacyl [*p*-Bu^t-calix[4]-(OMe)(O)₃Zr(Bu^tN=CPh)] (**23**), formed from the migratory insertion of Bu^tNC into the Zr–Ph in **22**. The proposed structures have been supported by X-ray analyses carried out on **4**, **6**, **13**, **16**, **22**, and **23**.

Introduction

The use of a preorganized O₄ set of oxygen donor atoms as a single ancillary ligand in organometallic chemistry does not have precedent, except for some very recent preliminary reports.^{1–3} The *p*-Bu^t-calix[4]arene and its alkylated forms⁴ (see Chart 1) allowed us to enter this new area.

The few previous reports concern exclusively the complexation of a transition metal ion by the calix[4]arene tetraanion

Chart 1



without any focus on the organometallic functionalization of the metal center.^{3ef,5} A, B, and C provide a coordination environment very different, in terms of geometry and coordination number, from that determined by the use of monodentate phenoxo groups. As shown in Chart 1, we can tune the charge of the calix macrocycle and, consequently, the degree of functionalization of the [O₄M] fragment *via* the alkylation of the calix[4]arene tetraanion. The major peculiarities in the use of A, B, or C (Chart 1) as ancillary ligands are (i) the calix[4]arene skeleton limits the adaptability of the O₄ set to certain

(5) (a) Zanotti-Gerosa, A.; Solari, E.; Giannini, L.; Floriani, C.; Chiesi-Villa, A.; Rizzoli, C. *Chem. Commun.* **1996**, 119. (b) Acho, J. A.; Ren, T.; Yun, J. W.; Lippard, S. J. *Inorg. Chem.* **1995**, *34*, 5226. (c) Acho, J. A.; Lippard, S. J. *Inorg. Chim. Acta* **1995**, *229*, 5. (d) Corazza, F.; Floriani, C.; Chiesi-Villa, A.; Rizzoli, C. *Inorg. Chem.* **1991**, *30*, 4465. (e) Corazza, F.; Floriani, C.; Chiesi-Villa, A.; Guastini, C. *J. Chem. Soc., Chem. Commun.* **1990**, 640. (f) Corazza, F.; Floriani, C.; Chiesi-Villa, A.; Guastini, C. *J. Chem. Soc., Chem. Commun.* **1990**, 1083. (g) Olmstead, M. M.; Sigel, G.; Hope, H.; Xu, X.; Power, P. P. *J. Am. Chem. Soc.* **1985**, *107*, 8087.

[†] Université de Lausanne.

[‡] Università di Parma.

[§] Università di Perugia.

[⊗] Abstract published in *Advance ACS Abstracts*, September 15, 1997.

(1) Giannini, L.; Solari, E.; Zanotti-Gerosa, A.; Floriani, C.; Chiesi-Villa, A.; Rizzoli, C. *Angew. Chem., Int. Ed. Engl.* **1996**, *35*, 85.

(2) Castellano, B.; Zanotti-Gerosa, A.; Solari, E.; Floriani, C.; Chiesi-Villa, A.; Rizzoli, C. *Organometallics* **1996**, *15*, 4894.

(3) (a) Giannini, L.; Solari, E.; Zanotti-Gerosa, A.; Floriani, C.; Chiesi-Villa, A.; Rizzoli, C. *Angew. Chem., Int. Ed. Engl.* **1996**, *35*, 2825. (b) Giannini, L.; Solari, E.; Zanotti-Gerosa, A.; Floriani, C.; Chiesi-Villa, A.; Rizzoli, C. *Angew. Chem., Int. Ed. Engl.*, in press. (c) Gardiner, M. G.; Lawrence, S. M.; Raston, C. L.; Skelton, B. W.; White, A. H. *Chem. Commun.* **1996**, 2491. (d) Gardiner, M. G.; Koutsantonis, G. A.; Lawrence, S. M.; Nichols, P. J.; Raston, C. L. *Chem. Commun.* **1996**, 2035. (e) Gibson, V. C.; Redshaw, C.; Clegg, W.; Elsegood, M. R. *J. Chem. Soc., Chem. Commun.* **1995**, 2371. (f) Acho, J. A.; Doerr, L. H.; Lippard, S. J. *Inorg. Chem.* **1995**, *34*, 2542.

(4) (a) Gutsche, C. D. *Calixarenes*; The Royal Society of Chemistry: Cambridge, U.K., 1989. (b) *Calixarenes, A Versatile Class of Macrocyclic Compounds*; Vicens, J.; Böhmer, V., Eds.; Kluwer: Dordrecht, The Netherlands, 1991.

arrangements around the metal, the square-planar being the favored one (such a geometrical constraint affects the M–O π bonding interaction and the frontier orbitals of the [O₄M] fragment) and (ii) methoxy groups in B and C can play the role of a spectator donor atom, thus adapting the coordination number requested by the metal along the reaction pathway.

The oxygen donor atoms are particularly appropriate for the oxophilic, early transition metals. We chose to investigate zirconium due to its relevant role in organic synthesis and catalysis.^{6–8} To this end, we took advantage of the contributions made by groups such as Rothwell and Wolczanski^{9,10} in using alkoxy functionalities as ancillary ligands in organometallic chemistry and catalysis assisted by early transition metals.

Herein we report full details on the synthesis and the chemical behavior of the Zr–C bond functionalities bonded to the O₄ skeleton shown in Chart 1 (see anions B and C). This approach has been developed through the synthesis and the organometallic functionalization of [calix[4]-(OMe)(O)₃ZrCl]₂ and [calix[4]-(OMe)₂(O)₂ZrCl]₂, which give rise to two classes of derivatives related by the base-induced demethylation of one of the methoxy groups. The experimental and theoretical studies reported here will emphasize the major differences between the [O₄Zr]²⁺, [O₄Zr]⁺, and [Cp₂Zr]²⁺ [Cp = η^5 -C₅H₅] fragments. The organometallic derivatization of [calix[4]-(OMe)₂(O)₂ZrCl]₂ has been briefly communicated.¹

(6) (a) Negishi, E.-I.; Takahashi, T. *Acc. Chem. Res.* **1994**, *27*, 124 and references therein. (b) Reetz, M. T. In *Organometallics in Synthesis*; Schlosser, M., Ed.; Wiley: New York, 1994; Chapter 3. (c) Erker, G.; Pfaff, R. *Organometallics* **1993**, *12*, 1921. (d) Negishi, E.-I. In *Comprehensive Organic Synthesis*; Paquette, L. A., Ed.; Pergamon: Oxford, 1991; Vol. 5, p 1163. (e) Schore, N. E. In *Comprehensive Organic Synthesis*; Paquette, L. A., Ed.; Pergamon: Oxford, 1991; Vol. 5, p 1037. (f) Buchwald, S. L.; Nielsen, R. B. *Chem. Rev.* **1988**, *88*, 1047.

(7) Cardin, D. J.; Lappert, M. F.; Raston, C. L. *Chemistry of Organozirconium and Hafnium Compounds*; Wiley: New York, 1986.

(8) (a) Ryan, E. J. In *Comprehensive Organometallic Chemistry II*; Abel, E. W., Stone, F. G. A., Wilkinson, G., Eds.; Pergamon: Oxford, 1995; Vol. 4, Chapter 9. (b) Coates, G. W.; Waymouth, R. M. In *Comprehensive Organometallic Chemistry II*; Abel, E. W., Stone, F. G. A., Wilkinson, G., Eds.; Pergamon: Oxford, 1995; Vol. 12, Chapter 12.1. (c) Jordan, R. F.; Lapointe, R. E.; Bradley, P. K.; Baenzinger, N. *Organometallics* **1989**, *8*, 2892 and references therein. (d) Buchwald, S. L.; La Maire, S. J.; Nielsen, R. B.; Watson, B. T.; King, S. M. *Tetrahedron Lett.* **1987**, *28*, 3895. (e) Neghishi, E.; Takahashi, T. *Aldrichim. Acta* **1985**, *18*, 31. (f) Neghishi, E.; Miller, J. A.; Yoshida, T. *Tetrahedron Lett.* **1984**, *25*, 3407. (g) Neghishi, E.; Yoshida, T. *Tetrahedron Lett.* **1980**, *21*, 1501. (h) Schwartz, J. *Pure Appl. Chem.* **1980**, *52*, 733. (i) Carr, D. B.; Yoshifujii, M.; Shoer, L. I.; Gell, K. I.; Schwartz, J. *Ann. N. Y. Acad. Sci.* **1977**, *295*, 127. (j) Schwartz, J.; Labinger, J. A. *Angew. Chem., Int. Ed. Engl.* **1976**, *15*, 333.

(9) Parkin, B. C.; Clark, J. R.; Visciglio, V. M.; Fanwick, P. E.; Rothwell, I. P. *Organometallics* **1995**, *14*, 3002. Clark, J. R.; Fanwick, P. E.; Rothwell, I. P. *J. Chem. Soc., Chem. Commun.* **1995**, 553. Bonanno, J. B.; Lobkovsky, E. B.; Wolczanski, P. T. *J. Am. Chem. Soc.* **1994**, *116*, 11159. Miller, R. L.; Toreki, R.; LaPointe, R. E.; Wolczanski, P. T.; Van Duyne, G. D.; Roe, D. C. *J. Am. Chem. Soc.* **1993**, *115*, 5570. Yu, J. S.; Ankianiec, B. C.; Rothwell, I. P.; Nguyen, M. T. *J. Am. Chem. Soc.* **1992**, *114*, 1927. Chesnut, R. W.; Jacob, G. G.; Yu, J. S.; Fanwick, P. E.; Rothwell, I. P. *Organometallics* **1991**, *10*, 321.

(10) (a) Zambrano, C. H.; Fanwick, P. E.; Rothwell, I. P. *Organometallics* **1994**, *13*, 1174. (b) Hill, J. E.; Baillich, G.; Fanwick, P. E.; Rothwell, I. P. *Organometallics* **1993**, *12*, 2911. (c) Baillich, G.; Fanwick, P. E.; Rothwell, I. P. *J. Am. Chem. Soc.* **1993**, *115*, 1581. (d) Hill, J. E.; Baillich, G.; Fanwick, P. E.; Rothwell, I. P. *Organometallics* **1991**, *10*, 3428. (e) Floriani, C.; Corazza, F.; Lesueur, W.; Chiesi-Villa, A.; Guastini, C. *Angew. Chem., Int. Ed. Engl.* **1989**, *28*, 66. (f) Chisholm, M. H.; Rothwell, I. P. In *Comprehensive Coordination Chemistry*; Wilkinson, G., Gillard, R. D., McCleverty, J. A., Eds.; Pergamon: Oxford, 1988; Vol. 2, Chapter 15.3. (g) Chamberlain, L. R.; Durfee, L. D.; Fau, P. E.; Fanwick, P. E.; Kobriger, L.; Latesky, S. L.; McMullen, A. K.; Rothwell, I. P.; Folting, K.; Huffman, J. C.; Streib, W. E.; Wang, R. *J. Am. Chem. Soc.* **1987**, *109*, 390, 6068 and references therein. (h) Durfee, L. D.; Fanwick, P. E.; Rothwell, I. P.; Folting, K.; Huffman, J. C. *J. Am. Chem. Soc.* **1987**, *109*, 4720. (i) Lubben, T. V.; Wolczanski, P. T. *J. Am. Chem. Soc.* **1987**, *109*, 424 and references therein. (j) Latesky, S. L.; McMullen, A. K.; Niccolai, G. P.; Rothwell, I. P. *Organometallics* **1985**, *4*, 902.

Experimental Section

All operations were carried out under an atmosphere of purified nitrogen. All solvents were purified by standard methods and freshly distilled prior to use. NMR spectra were recorded on 200-AC and 400-dpx Bruker instruments. The syntheses of **1** and **2** have been performed as reported in the literature.¹¹

Synthesis of 4. BuLi (69 mL, 1.65 M in hexane, 114 mmol) was added dropwise over 30 min to a stirred solution of **2** (39.3 g, 58.0 mmol) in THF (400 mL). The resulting orange solution was transferred to a dropping funnel and added dropwise to a suspension of ZrCl₄·(thf)₂ (22.6 g, 60.0 mol) in THF (200 mL), yielding a yellow solution. Volatiles were removed *in vacuo*, the flask was charged with fresh benzene (400 mL), and the reaction mixture was refluxed for 3 h. The mixture was stirred overnight and then extracted over 12 h. Volatiles were removed *in vacuo*, benzene (400 mL) was added, and the mixture was extracted over 2 h, to yield a white suspension. Volatiles were removed *in vacuo*, benzene (100 mL) and hexane (300 mL) were then added, and the mixture was stirred for 5 h. The white microcrystalline **4**·(C₆H₆)₂ was collected and dried *in vacuo* (43.07 g, 75%). ¹H NMR (CD₂Cl₂, 298 K): δ 7.37 (s, 12H, benzene), 7.16 (s, 4H, ArH), 7.11 (s, 4H, ArH), 4.53 (s, 6H, MeO), 4.34 (d, J = 13.0 Hz, 4H, *endo*-CH₂), 3.44 (d, J = 13.0 Hz, 4H, *exo*-CH₂), 1.30 (s, 18H, Bu^t), 1.17 (s, 18H, Bu^t). Anal. Calcd for **4**·(C₆H₆)₂, C₅₈H₇₀Cl₂O₄Zr: C, 70.13; H, 7.10. Found: C, 70.12, H, 7.44. Crystals suitable for X-ray analysis were obtained at room temperature from supersaturated benzene solutions of **4**.

Synthesis of 5. Et₃N (1 mL) was added at room temperature to a solution of **4**·(C₆H₆)₂ (1.61 g, 1.62 mmol) in toluene (100 mL), yielding a white suspension. **5**·(C₇H₈)₂ was collected as a white powder (1.14 g, 65%). ¹H NMR (CD₂Cl₂, 298 K): δ 7.22 (m, 10H, C₇H₈), 7.04 (m, 6H, ArH), 6.94 (m, 2H, ArH), 4.53 (d, J = 12.6 Hz, 2H, *endo*-CH₂), 4.33 (d, J = 12.6 Hz, 2H, *endo*-CH₂), 4.26 (s, 3H, MeO), 3.38 (m, 6H, CH₂), 3.25 (d, J = 12.6 Hz, 2H, *exo*-CH₂), 3.12 (d, J = 12.6 Hz, 2H, *exo*-CH₂), 3.01 (s, 3H, CH₃), 2.34 (s, 6H, C₇H₈), 1.35 (m, 9H, CH₃), 1.26 (s, 9H, Bu^t), 1.15 (s, 9H, Bu^t), 1.34 (s, 18H, Bu^t). Anal. Calcd for **5**·(C₇H₈)₂, C₆₃H₈₃Cl₂NO₄Zr: C, 70.03; H, 7.74; N, 1.30. Found: C, 69.82; H, 8.12; N, 1.10.

Hydrolysis of 5. **5** (0.074 g, 72.0 mmol) was dissolved in CH₂Cl₂ (10 mL) under an N₂ atmosphere and hydrolyzed with diluted HCl. The organic layer was washed with water (3 × 7 mL) and dried (Na₂SO₄, then *in vacuo*). Clean **8** resulted as determined by ¹H NMR analysis (CDCl₃). Analogous results were obtained on reacting **4**·(C₆H₆)₂ with pyridine; such a treatment, followed by hydrolysis, gave clean **8**.

Synthesis of 6. AgOTf (1.07 g, 4.16 mmol) was added to a benzene (100 mL) solution of **4**·(C₆H₆)₂ (2.1 g, 2.1 mmol). A white, fluffy solid formed, and the mixture was stirred overnight. Salts were filtered off, benzene was almost completely removed *in vacuo*, and hexane (80 mL) was added. The white mixture was briefly refluxed and then extracted for 3 h (some dark solid was left on the frit, filtration in benzene does not completely remove Ag salts). Keeping the resulting colorless solution at –25 °C for 12 h gave **6**·C₆H₆ as a white microcrystalline solid, which was collected and dried *in vacuo* (1.58 g, 66%). ¹H NMR (C₆D₆, 298 K): δ 7.17 (s, 4H, ArH), 6.76 (s, 4H, ArH), 4.54 (d, J = 12.9 Hz, 4H, *endo*-CH₂), 3.89 (s, 6H, MeO), 3.23 (d, J = 12.9 Hz, 4H, *exo*-CH₂), 1.36 (s, 18H, Bu^t), 0.65 (s, 18H, Bu^t). Anal. Calcd for **6**·C₆H₆: C₅₄H₆₄F₆O₁₀S₂Zr: C, 56.77; H, 5.65. Found: C, 56.72; H, 5.44. Crystals suitable for X-ray analysis were obtained at room temperature from a supersaturated solution of **6**·C₆H₆ in hexane. The product is thermally stable in C₆D₆ (14 h, 65 °C) and polymerizes THF. **6** reacted with pyridine to give **7**, as was observed in an NMR tube. The hydrolysis of **7** gave clean **8**.

Synthesis of 8. **2** (41.0 g, 60.7 mmol) and TiCl₄·(thf)₂ (20.2 g, 60.6 mmol) were dissolved in toluene (500 mL). The dark red solution was refluxed for 4 days. HCl (10% water solution, 300 mL) was added and the mixture stirred overnight. The organic layer was extracted, washed with water until neutrality (3 × 300 mL), dried (Na₂SO₄), and filtered. The solvent was removed *in vacuo* at the diffusive pump (130 °C, 8 h), yielding **8** as a white powder (35.6 g, 89%). ¹H NMR (CDCl₃,

(11) Arduini, A.; Casnati, A. In *Macrocyclic Synthesis*; Parker, O., Ed.; Oxford University Press: New York, 1996; Chapter 7.

298 K): δ 10.16 (br s, 1H, Ar-OH), 9.58 (br s, 2H, ArOH), 7.11 (s, 2H, ArH), 7.07 (m, 4H, ArH), 7.00 (m, 2H, ArH), 4.37 (d, $J = 13.7$ Hz, 2H, *endo*-CH₂), 4.32 (d, $J = 13.7$ Hz, 2H, *endo*-CH₂), 4.14 (s, 3H, MeO), 3.43 (d, $J = 13.7$ Hz, 2H, *exo*-CH₂), overlapping with 3.43 (d, $J = 13.7$ Hz, 2H, *exo*-CH₂), 1.23 (s, 18H, Bu^t), 1.22 (s, 9H, Bu^t), 1.21 (s, 9H, Bu^t). Anal. Calcd for **8**, C₄₅H₅₈O₄: C, 81.53; H, 8.82. Found: C, 81.20; H, 8.77.

Synthesis of 9. BuLi (20.4 mL, 1.79 M in *n*-hexane, 36.5 mmol) was added dropwise over 1 h to a stirred solution of **8** (8.07 g, 12.2 mmol) in toluene (180 mL) kept at 16 °C. The reaction mixture was refluxed over 2 h. Volatiles were removed *in vacuo*, and hexane (150 mL) was added to the residue. **9** was collected as a white powder (7.24 g, 87%). ¹H NMR (CD₂Cl₂, 298 K): δ 7.10 (d, $J = 2.4$ Hz, 2H, ArH), 7.06 (d, $J = 2.4$ Hz, 2H, ArH), 6.85 (s, 2H, ArH), 6.78 (s, 2H, ArH), 4.31 (d, $J = 13.2$ Hz, 2H, *endo*-CH₂), 3.99 (d, $J = 14.2$ Hz, 2H, *endo*-CH₂), 3.74 (s, 3H, MeO), 3.29 (d, $J = 14.2$ Hz, 2H, *exo*-CH₂), overlapping with 3.28 (d, $J = 13.2$ Hz, 2H, *exo*-CH₂), 1.29 (s, 18H, Bu^t), 1.02 (s, 9H, Bu^t), 0.95 (s, 9H, Bu^t). Anal. Calcd for **9**, C₄₅H₅₅O₄·Li₃: C, 79.40; H, 8.14. Found: C, 79.48; H, 8.23.

Synthesis of 10. **9** (14.0 g, 20.5 mmol) and ZrCl₄·(thf)₂ (7.85 g, 20.8 mmol) were suspended in benzene (180 mL). The reaction mixture was refluxed for 16 h and then extracted for 48 h. Volatiles were then removed *in vacuo*, and hexane (80 mL) was added to the residue. **10**·2(thf)·2C₆H₆ was collected as a white powder (15.76 g, 82%). ¹H NMR (pyr-*d*₅, 298 K): δ 7.48 (d, $J = 2.4$ Hz, 4H, ArH), 7.37 (d, $J = 2.4$ Hz, 4H, ArH), 7.34 (s, 12H, C₆H₆), 7.03 (s, 4H, ArH), 6.85 (s, 4H, ArH), 4.96 (d, $J = 12.2$ Hz, 4H, *endo*-CH₂), 4.66 (d, $J = 12.2$ Hz, 4H, *endo*-CH₂), 3.91 (s, 6H, MeO), 3.62 (m, 8H, THF), 3.54 (d, $J = 12.2$ Hz, 4H, *exo*-CH₂), 3.19 (d, $J = 12.2$ Hz, 4H, *exo*-CH₂), 1.59 (m, 8H, THF), 1.46 (s, 36H, Bu^t), 0.85 (s, 18H, Bu^t), 0.78 (s, 18H, Bu^t). Anal. Calcd for **10**·2(thf)·2C₆H₆, C₁₁₀H₁₃₈Cl₂O₁₀Zr₂: C, 70.52; H, 7.42. Found: C, 70.45; H, 7.63.

Synthesis of 11. **10**·2(thf)·2C₆H₆ (3.17 g, 1.69 mmol) was treated with pyridine to give a turbid solution, which was filtered. The resulting colorless solution was kept at -24 °C for 2 days to give colorless crystals of **11**·3(Py) and then dried *in vacuo*. ¹H NMR: (pyr-*d*₅, 298 K): δ 7.60–7.16 (ArH), 4.97 (d, $J = 12.2$ Hz, 2H, *endo*-CH₂), 4.69 (d, $J = 12.7$ Hz, 2H, *endo*-CH₂), 3.93 (s, 3H, MeO), 3.55 (d, $J = 12.2$ Hz, 2H, *exo*-CH₂), 3.21 (d, $J = 12.7$ Hz, 2H, *exo*-CH₂), 1.47 (s, 18H, Bu^t), 0.86 (s, 9H, Bu^t), 0.79 (s, 9H, Bu^t). Anal. Calcd for C₇₀H₈₀·CIN₅O₄Zr: C, 71.12; H, 6.82; N, 5.92. Found: C, 71.04; H, 6.67; N, 6.20. Crystals with formula **11**·(Py)_{6.5} were obtained at -24 °C from a room temperature saturated solution of **10**·(thf)₂·(C₆H₆)₂ in pyridine.

Synthesis of 12. Method A. **2** (20.8 g, 30.8 mmol) and ZrCl₄·(thf)₂ (11.4 g, 30.3 mmol) were suspended in benzene (200 mL), and the reaction mixture was refluxed for 2 h. The solvent was distilled off and then added again. After a further 10 min reflux, the solvent was evaporated to dryness and the residue dried *in vacuo* at 80 °C. The flask was then charged with fresh benzene (300 mL), and to the stirred mixture was added MeLi (30.3 mL, 2.0 M in Et₂O, 60.6 mmol) dropwise over 1 h, resulting in a yellow suspension. The mixture was concentrated to ~30 mL and *n*-hexane (250 mL) added to the yellow, creamy suspension. Extraction over 48 h gave a colorless powder of **12**, which was then collected by filtration and finally dried *in vacuo* (10.9 g, 45%). Colorless crystals of **12**·(C₆H₆)₂ were collected from the mothers liquor kept at -18 °C for 2 days (6.48 g, 22.5%). ¹H NMR (C₆D₆, 298 K): δ 7.23 (s, 4H, ArH), 6.80 (s, 4H, ArH), 4.46 (d, $J = 12.5$ Hz, 4H, *endo*-CH₂), 3.69 (s, 6H, MeO), 3.18 (d, $J = 12.5$ Hz, 4H, *exo*-CH₂), 1.46 (s, 18H, Bu^t), 1.25 (s, 6H, Me-Zr), 0.77 (s, 18H, Bu^t). Anal. Calcd for **12**, C₄₈H₆₄O₄Zr: C, 72.41; H, 8.10. Found: C, 71.94; H, 8.35.

Method B. MeLi (7.7 mL, 1.71 M in Et₂O, 13.2 mmol) was added dropwise to a toluene (200 mL) solution of **4**·(C₆H₆)₂ (6.6 g, 6.7 mmol) at -30 °C. The mixture was allowed to warm to room temperature with stirring, and then volatiles were removed *in vacuo*, benzene (150 mL) was added, and the mixture was heated to reflux, filtered while hot, and concentrated *in vacuo* by evaporation to ca. 30 mL. *n*-Hexane (200 mL) was added to the resulting white, creamy suspension and the mixture refluxed to give a colorless solution. Standing at 9 °C for 3 days gave colorless crystals of **12**·C₆H₆, which were collected and dried *in vacuo* (3.66 g, 63%). ¹H NMR (CD₂Cl₂, 298 K): δ 7.36 (s, 6H, benzene), 7.10 (s, 4H, ArH), 6.96 (s, 4H, ArH), 4.42 (d, $J = 12.5$ Hz,

4H, *endo*-CH₂), 4.22 (s, 6H, MeO), 3.32 (d, $J = 12.5$ Hz, 4H, *exo*-CH₂), 1.27 (s, 18H, Bu^t), 1.07 (s, 18H, Bu^t), 0.62 (s, 6H, Me-Zr). Anal. Calcd for **12**·C₆H₆, C₅₄H₇₀O₄Zr: C, 74.18; H, 8.07. Found: C, 74.38; H, 8.18. Crystals suitable for X-ray analysis were obtained by keeping a pentane solution of **12** saturated at room temperature at 8 °C. The product is stable to prolonged heating (65 °C, 14 h) in C₆D₆ and CD₂Cl₂, as judged by ¹H NMR; it is not photosensitive in C₆D₆ but gives **4** when photolyzed in CD₂Cl₂. The redistribution reaction between **12** and **4** is fast; dissolving the two compounds (ca. 20 mg of each) in ca. equimolar amounts in CD₂Cl₂ gives an equilibrium mixture of the two reagents and a new product in ca. 1:1:2 ratio, as judged by ¹H NMR [for the new species, δ 7.13 (s, 4H, ArH), 7.04 (s, 4H, ArH), 4.43 (d, $J = 12.5$ Hz, 4H, *endo*-CH₂), 4.36 (s, 6H, MeO), 3.37 (d, $J = 12.5$ Hz, 4H, *exo*-CH₂), 1.27 (s, 18H, Bu^t), 1.13 (s, 18H, Bu^t), 0.82 (s, 3H, Me-Zr)]. Some peaks overlap with those of the two reagents.

Synthesis of 13. Method A. **2** (26.2 g, 39.0 mmol) and ZrCl₄·(thf)₂ (14.5 g, 38.4 mmol) were suspended in benzene (200 mL), and the reaction mixture was refluxed for 2 h. The solvent was removed by distillation and then added again. After a further reflux (10 min), the solvent was removed by distillation and the residue dried *in vacuo* at 80 °C. The flask was then charged with fresh toluene (200 mL), and to the stirred mixture, at -30 °C, was added a solution of CH₂-PhMgCl (118.0 mL, 0.68 M in THF, 80 mmol) dropwise over 45 min. The mixture, which became bright yellow in seconds, was allowed to warm to room temperature. Dioxane (20 mL) was added, and the mixture was stirred over 1 h. Volatiles were removed *in vacuo* (heating to 80 °C over 2 h). The residue was extracted over 3 days with a mixture of *n*-hexane (500 mL) and benzene (100 mL), to give a yellow suspension. The bright yellow microcrystalline **13** was collected and dried *in vacuo* (12.0 g, 33%). A further extraction of the solid left on the extractor with benzene (250 mL) resulted in the collection of **13**·(C₆H₆)₂ light yellow powder (10.8 g, 25.4%). Anal. Calcd for **13**·(C₆H₆)₂, C₇₂H₈₄O₄Zr: C, 78.27; H, 7.66. Found: C, 78.25; H, 8.07.

Method B. PhCH₂MgCl (34 mL, 1.33 M in THF, 45.2 mmol) was added dropwise to a toluene (300 mL) solution of **4**·(C₆H₆)₂ (22.75 g, 22.9 mmol) at -35 °C. The mixture, which became bright yellow in seconds, was allowed to warm to room temperature with stirring. Dioxane (10 mL) was added, and the mixture was stirred for 1 h. Volatiles were removed *in vacuo* (heating to 50 °C). The residue was extracted over 3 days with a mixture of hexane (500 mL) and benzene (60 mL), yielding a yellow suspension. The microcrystalline, bright yellow **13** was collected and dried *in vacuo* (16.8 g, 77%). ¹H NMR (CD₂Cl₂, 298 K): δ 7.34–7.17 (m, 8H, ArH(CH₂Ph)), 7.12 (s, 4H, ArH), 7.00 (s, 4H, ArH), 6.85 (m, 2H, ArH(CH₂Ph)), 4.28 (d, $J = 12.5$ Hz, 4H, *endo*-CH₂), 3.60 (s, 6H, MeO), 3.27 (d, $J = 12.5$ Hz, 4H, *exo*-CH₂), 2.69 (s, 4H, CH₂Ph), 1.28 (s, 18H, Bu^t), 1.12 (s, 18H, Bu^t). ¹H NMR (C₆D₆, 298 K): δ 7.65 (m, 4H, ArH(CH₂Ph)), 7.31 (s, 4H, ArH), 7.23 (m, 4H, ArH(CH₂Ph)), 6.86 (m, 2H, ArH(CH₂Ph)), 6.80 (s, 4H, ArH), 4.46 (d, $J = 12.5$ Hz, 4H, *endo*-CH₂), 3.37 (s, 6H, MeO), 3.24 (d, $J = 12.5$ Hz, 4H, *exo*-CH₂), 3.04 (s, 4H, CH₂Ph), 1.45 (s, 18H, Bu^t), 0.70 (s, 18H, Bu^t). Anal. Calcd for **13**, C₆₀H₇₂O₄Zr: C, 75.98; H, 7.65. Found: C, 76.21; H, 7.73. Crystals suitable for X-ray analysis were obtained at room temperature from a supersaturated solution of **13** in toluene. The product is thermally stable (65 °C, 14 h) in C₆D₆ and CD₂Cl₂, as judged by ¹H NMR. It is photosensitive; exposing C₆D₆ solutions of the product to solar light for a few hours gives quantitatively the PhCH₂-CH₂Ph coupling product (¹H NMR), together with a lower symmetry calixarene species.

Synthesis of 14. LiCH₂SiMe₃ (1.07 g, 11.4 mmol) was added to a suspension of **4**·(C₆H₆)₂ (5.63 g, 5.67 mmol) in toluene (150 mL) kept at -40 °C. The reaction mixture was allowed to warm to room temperature under stirring overnight. Volatiles were removed *in vacuo*, and Et₂O (150 mL) was added to the residue, which was extracted for 3 h to yield a white powder of **14** (2.92 g, 55%). ¹H NMR (C₆D₆, 298 K): δ 7.24 (s, 4H, ArH), 6.82 (s, 4H, ArH), 4.58 (d, $J = 12.2$ Hz, 4H, *endo*-CH₂), 3.81 (s, 6H, MeO), 3.30 (d, $J = 12.2$ Hz, 4H, *exo*-CH₂), 1.40 (s, 18H, Bu^t), 1.23 (s, 4H, CH₂), 0.80 (s, 18H, Bu^t), 0.48 (s, 18H, SiMe₃). Anal. Calcd for **14**, C₅₄H₈₀O₄Si₂Zr: C, 68.95; H, 8.53. Found: C, 69.10; H, 8.85. The product is stable to prolonged heating (80 °C, 14 h) in C₆D₆, as judged by NMR. Decomposition of the product was observed under photolysis (313 nm, 3 h) in C₆D₆.

Synthesis of 15. Method A. **2** (14.2 g, 21.0 mmol) and $\text{ZrCl}_4 \cdot (\text{thf})_2$ (7.83 g, 20.7 mmol) were suspended in benzene (200 mL), and the reaction mixture was refluxed for 2 h. The solvent was removed by distillation and then readded. After a further reflux of 10 min, the solvent was removed by distillation, and the residue was dried *in vacuo* at 80 °C. The flask was then charged with fresh toluene (250 mL), and to the stirred mixture was added *p*- $\text{MeC}_6\text{H}_4\text{MgBr}$ (41.6 mL, 1 M in THF, 41.6 mmol) dropwise over 1 h, resulting in a yellow suspension. The mixture was stirred for 3 h at room temperature, and then dioxane (10 mL) was added and stirring continued for 1 h. The white salts were filtered off and washed with toluene (150 mL). Volatiles were removed *in vacuo*. *n*-Hexane (150 mL) was added to the residue, and **15** was collected as a white powder (15.5 g, 78%). $^1\text{H NMR}$ (C_6D_6 , 298 K): δ 8.14 (d, $J = 7.4$ Hz, 4H, ArH(*p*-tolyl)), 7.27 (s, 4H, ArH), 7.12 (d, $J = 7.4$ Hz, 4H, ArH(*p*-tolyl)), 6.79 (s, 4H, ArH), 4.60 (d, $J = 12.5$ Hz, 4H, *endo*- CH_2), 3.35 (s, 6H, MeO), 3.19 (d, $J = 12.5$ Hz, 4H, *exo*- CH_2), 2.22 (s, 6H, CH_3 (*p*-tolyl)), 1.44 (s, 18H, Bu^t), 0.84 (s, 18H, Bu^t). Anal. Calcd for **15**, $\text{C}_{60}\text{H}_{72}\text{O}_4\text{Zr}$: C, 75.98; H, 7.65. Found: C, 75.72; H, 7.73.

Method B. *p*- $\text{MeC}_6\text{H}_4\text{MgBr}$ (10 mL, 0.98 M in THF, 9.8 mmol) was added dropwise to a toluene (50 mL) solution of **4** (C_6H_6)₂ (4.81 g, 4.84 mmol). Dioxane (2 mL) was added to the resulting cloudy solution, and the mixture was stirred overnight. The salts were filtered off, and volatiles were removed *in vacuo*. *n*-Hexane (40 mL) was added to the residue, the flask kept at –24 °C overnight, and the white **15** was finally collected and dried *in vacuo* (3.02 g, 65.4%). Anal. Calcd for **15**, $\text{C}_{60}\text{H}_{72}\text{O}_4\text{Zr}$: C, 75.98, H, 7.65. Found: C, 76.23; H, 7.77.

Synthesis of 16. **15** (3.75 g, 3.96 mmol) was dissolved in benzene (130 mL) and the colorless solution refluxed for 36 h to give an orange-brown solution. Volatiles were removed *in vacuo*, and *n*-hexane (30 mL) was added to the residue. The resulting **16** was collected as a white powder (1.55 g, 46%). $^1\text{H NMR}$ (C_6D_6 , 298 K): δ 8.05 (d, $J = 6.8$ Hz, 1H, ArH), 7.91 (s, 1H, ArH), 7.59 (d, $J = 6.8$ Hz, 1H, ArH), 7.24 (s, 4H, ArH), 6.87 (s, 4H, ArH), 4.62 (s, 6H, MeO) 4.48 (d, $J = 12.2$ Hz, 4H, *endo*- CH_2), 3.23 (d, $J = 12.2$ Hz, 4H, *exo*- CH_2), 2.60 (s, 3H, CH_3), 1.44 (s, 18H, Bu^t), 0.78 (s, 18H, Bu^t). Anal. Calcd for **16**, $\text{C}_{53}\text{H}_{64}\text{O}_4\text{Zr}$: C, 74.34; H, 7.53. Found: C, 74.49; H, 7.95. Crystals suitable for X-ray analysis were obtained from a saturated toluene solution of **16** at 8 °C. The product is stable to prolonged heating (120 °C, 14 h) in toluene, as determined by $^1\text{H NMR}$.

Synthesis of 17. $(\text{CH}_2\text{Ph})_2\text{Mg}$ (4.7 mL, 0.35 M in Et₂O, 1.65 mmol) was added dropwise over 30 min to a stirred toluene solution (80 mL) of **10** ($(\text{thf})_2(\text{C}_6\text{H}_6)_2$) (3.08 g, 1.64 mmol) kept at –30 °C. The mixture, which became a yellow suspension in seconds, was allowed to warm to room temperature. Dioxane (2 mL) was added, and the mixture was refluxed over 2 h and filtered. Volatiles were removed *in vacuo*, *n*-hexane (30 mL) was added to the residue, and **17** was collected as a pale yellow powder (1.2 g, 43%). $^1\text{H NMR}$ (C_6D_6 , 298 K): δ 7.41 (m, 4H, ArH), 7.28 (m, 4H, ArH), overlapping with 7.26 (d, $J = 2.4$ Hz, 4H, ArH), 7.22 (d, $J = 2.4$ Hz, 4H, ArH), 6.99 (m, 2H, ArH), 6.87 (s, 4H, ArH), 6.82 (s, 4H, ArH), 4.86 (d, $J = 12.7$ Hz, 4H, *endo*- CH_2), 4.32 (d, $J = 12.2$ Hz, 4H, *endo*- CH_2), 3.49 (s, 6H, MeO), 3.31 (d, $J = 12.7$ Hz, 4H, *exo*- CH_2), overlapping with 3.25 (d, $J = 12.2$ Hz, 4H, *exo*- CH_2), 2.86 (s, 4H, CH_2Ph), 1.41 (s, 36H, Bu^t), 0.80 (s, 18H, Bu^t), 0.69 (s, 18H, Bu^t). $^1\text{H NMR}$ (pyr-*d*₅, 298 K): δ 7.51–6.74 (ArH), 4.80 (d, $J = 12.0$ Hz, 2H, *endo*- CH_2), 4.55 (d, $J = 12.5$ Hz, 2H, *endo*- CH_2), 4.15 (s, 3H, MeO), 3.59 (d, $J = 12.0$ Hz, 2H, *exo*- CH_2), 3.26 (d, $J = 12.5$ Hz, 2H, *exo*- CH_2), 2.79 (s, 2H, CH_2Ph), 1.46 (s, 18H, Bu^t), 0.80 (s, 9H, Bu^t), 0.79 (s, 9H, Bu^t). Anal. Calcd for **17**, $\text{C}_{104}\text{H}_{124}\text{O}_8\text{Zr}_2$: C, 74.15; H, 7.42. Found: C, 73.16; H, 7.61. Rather clean **17** ($^1\text{H NMR}$, C_6D_6) was obtained by refluxing overnight a THF (100 mL) solution of **13** (2.0 g) and Et₃N (1.0 mL). Gas–mass chromatographical analysis of the reaction mixture revealed the presence of ethylene, toluene, and ethylbenzene.

Synthesis of 18. **13** (3.12 g, 3.29 mmol) was dissolved at room temperature in pyridine (60 mL), and the resulting yellow solution was allowed to stand for 36 h at room temperature in the dark. Volatiles were then removed *in vacuo*, and hexane (60 mL) was added to the residue. The resulting yellow solution was kept at 9 °C for 24 h, yielding a pale yellow solid, which was collected, washed with hexane (2 × 15 mL), and dried *in vacuo* (2.24 g, 74%). $^1\text{H NMR}$ (pyr-*d*₅, 298 K): δ 7.48 (d, $J = 2.3$ Hz, 2H, ArH), 7.42 (d, $J = 2.3$ Hz, 2H,

ArH), 7.17 (m, 2H, ArH(CH_2Ph)), 7.07 (s, 2H, ArH), 6.97 (m, 1H, ArH(CH_2Ph)), 6.85 (s, 2H, ArH), 6.75 (m, 2H, ArH(CH_2Ph)), 4.78 (d, $J = 12.1$ Hz, 2H, *endo*- CH_2), 4.54 (d, $J = 12.5$ Hz, 2H, *endo*- CH_2), 4.14 (s, 3H, MeO), 3.58 (d, $J = 12.1$ Hz, 2H, *exo*- CH_2), 3.25 (d, $J = 12.5$ Hz, 2H, *exo*- CH_2), 2.78 (s, 2H, CH_2Ph), 1.45 (s, 18H, Bu^t), 0.79 (s, 9H, Bu^t), overlapping with 0.78 (s, 9H, Bu^t). $^1\text{H NMR}$ (C_6D_6 , 298 K): δ 8.70 (m, 2H, pyr), 7.30 (d, $J = 2.4$ Hz, 2H, ArH), 7.28 (d, $J = 2.4$ Hz, 2H, ArH), 7.13 (m, 2H, ArH(CH_2Ph)), 6.97–6.80 (m, 8H, ArH, pyr, CH_2Ph), 6.60 (m, 2H, pyr), 4.63 (d, $J = 12.1$ Hz, 2H, *endo*- CH_2), overlapping with 4.56 (br d, 2H, *endo*- CH_2), 3.75 (s, 3H, MeO), 3.40 (d, $J = 12.1$ Hz, 2H, *exo*- CH_2), 3.24 (d, $J = 12.6$ Hz, 2H, *exo*- CH_2), 2.62 (br s, 2H, CH_2Ph), 1.43 (s, 18H, Bu^t), 0.81 (s, 9H, Bu^t), 0.78 (s, 9H, Bu^t). Anal. Calcd for **18**, $\text{C}_{57}\text{H}_{67}\text{NO}_4\text{Zr}$: C, 74.30; H, 7.33; N, 1.52. Found: C, 74.48; H, 7.69; N, 1.69. The product is thermally stable (65 °C, 14 h) in C_6D_6 , as judged by $^1\text{H NMR}$. It is not photosensitive. When hydrolyzed, clean **8** is obtained. The demethylation pathway is supported by the following observations: (i) The reaction was conducted in pyr-*d*₅, volatiles were removed *in vacuo*, and the residue was dissolved in C_6D_6 . $^1\text{H NMR}$ showed clean **18** plus three resonances at δ 2.73 (br d), 2.24 (s), and 2.16 (s). (ii) $(\text{CH}_2\text{Ph})_2\text{Mg}$ (1.8 mL, 1.17 N, 2.10 mequiv) was added at –40 °C to a suspension of $\text{PyMe}^+\text{BPh}_4^-$ (0.932 g, 2.25 mmol) in THF (100 mL), and the mixture was allowed to stir at room temperature. A sample of the resulting solution was evaporated to dryness, and the residue was dissolved in C_6D_6 . $^1\text{H NMR}$ revealed resonances at δ 5.99 (m), 5.73 (m), 5.45 (m), 4.88 (m), 4.42 (m), 3.82 (m), 3.47 (m), 2.75 (m), 2.24 (s), and 2.16 (s). (iii) A sample of the pyridine reaction mixture, before workup with *n*-hexane, was evaporated to dryness and the residue dissolved in C_6D_6 . $^1\text{H NMR}$ showed clean **8**, plus resonances at δ 5.99 (m), 5.73 (m), 5.45 (m), 4.88 (m), 4.42 (m), 3.82 (m), 3.47 (m), overlapping with one of the CH_2 doublets of **18**, 2.75 (m), 2.24 (s), and 2.16 (s).

Synthesis of 19. $[\text{Cp}_2\text{Fe}]^+\text{BPh}_4^-$ (1.35 g, 2.40 mmol) was added to a suspension of **13** (2.06 g, 2.17 mmol) in toluene (100 mL) at –35 °C, and the mixture was warmed to room temperature over 5 h; at this temperature, all of the $[\text{Cp}_2\text{Fe}]^+\text{BPh}_4^-$ had disappeared and a yellow suspension resulted. It was stirred overnight, and then the bright yellow, microcrystalline **19** (C_7H_8) was collected, washed with hexane (2 × 20 mL), and dried *in vacuo* (0.86 g, 31%). $^1\text{H NMR}$ (CD_2Cl_2 , 298 K): δ 7.73–6.82 (m, 38H, ArH), 4.18 (d, $J = 12.9$ Hz, 4H, *endo*- CH_2), 3.74 (s, 6H, MeO), 3.45 (d, $J = 12.9$ Hz, 4H, *exo*- CH_2), overlapping with 3.40 (s, 2H, CH_2Ph), 2.34 (s, 3H, C_7H_8) 1.30 (s, 18H, Bu^t), 0.99 (s, 18H, Bu^t). Anal. Calcd for **19** (C_7H_8), $\text{C}_{84}\text{H}_{93}\text{BO}_4\text{Zr}$: C, 79.52; H, 7.39. Found: C, 78.99; H, 7.73. The product is thermally unstable in C_6D_6 (1 h, 90 °C), giving **13** and a dimeric **22** ($^1\text{H NMR}$, X-ray). It is unstable in CD_2Cl_2 (at room temperature, the product disappears in days). It is photosensitive. It reacts with THF to give the adduct ($^1\text{H NMR}$, <10 min); coordinated THF is labile, as shown by the fact that, in the presence of more than 1 THF *per* Zr, a single set of THF signals is visible, at chemical shifts strongly dependent on the amount of THF and falling in between those of free and coordinated THF. **19** (C_7H_8) reacts with pyridine to give $\text{PyMe}^+(\text{BPh}_4)^-$ and **18** ($^1\text{H NMR}$). It does not react with ethylene.

Synthesis of 20. $[\text{Cp}_2\text{Fe}]^+\text{BPh}_4^-$ (0.82 g, 1.62 mmol) was added to a solution of **13** (1.44 g, 1.52 mmol) in THF (100 mL) at –35 °C, and the mixture was warmed to room temperature over 3 h; at this temperature, all of the $[\text{Cp}_2\text{Fe}]^+\text{BPh}_4^-$ had disappeared, and a yellow solution was obtained. Volatiles were removed *in vacuo*, and the residue was washed with pentane (75 mL), collected, and dried *in vacuo* (1.3 g). $^1\text{H NMR}$ and elemental analyses revealed that the product was impure due to polymeric THF; analytically pure **20** (1.0 g, 52.7%) was obtained by recrystallization of the crude product in benzene/hexane (60/90 mL). $^1\text{H NMR}$ (CD_2Cl_2 , 298 K): δ 7.60–6.85 (m, 33H, ArH), 4.31 (m, 4H, THF), 4.14 (d, $J = 12.9$ Hz, 4H, *endo*- CH_2), 3.76 (s, 6H, MeO), 3.44 (d, $J = 12.9$ Hz, 4H, *exo*- CH_2), 3.02 (s, 2H, CH_2Ph), 2.08 (m, 4H, THF), 1.30 (s, 18H, Bu^t), 1.09 (s, 18H, Bu^t). Anal. Calcd for **20**, $\text{C}_{81}\text{H}_{93}\text{BO}_5\text{Zr}$: C, 77.91; H, 7.51. Found: C, 77.58; H, 7.49.

Synthesis of 21. A solution of $\text{B}(\text{C}_6\text{F}_5)_3$ (1.03 g, 2.01 mmol) in toluene (50 mL) was added dropwise to a suspension of **13** (1.93 g, 2.03 mmol) in toluene (150 mL), giving a yellow solution. Volatiles were removed *in vacuo*, and the residue was washed with hexane (100 mL), collected, and dried *in vacuo* (2.65 g, 89.4%). $^1\text{H NMR}$

Table 1. Experimental Data for the X-ray Diffraction Studies on Crystalline Complexes **13**, **16**, **22** and **23**

	13	16	22	23
formula	C ₆₀ H ₇₂ O ₄ Zr·C ₇ H ₈	C ₅₃ H ₆₄ O ₄ Zr·0.75C ₇ H ₈	C ₁₀₂ H ₁₂₀ O ₈ Zr ₂ ·C ₆ H ₆	C ₅₆ H ₆₉ NO ₄ Zr·C ₆ H ₆ ·C ₆ H ₁₄
color	pale yellow	colorless	colorless	colorless
<i>a</i> , Å	23.354(1)	19.925(4)	11.009(2)	12.982(3)
<i>b</i> , Å	20.518(2)	20.119(4)	12.358(2)	28.958(6)
<i>c</i> , Å	13.238(1)	14.545(3)	19.990(2)	18.424(4)
α, deg	90	100.82(3)	73.35(1)	90
β, deg	112.77(1)	99.74(3)	87.36(1)	110.42(3)
γ, deg	90	63.52(2)	70.17(1)	90
<i>V</i> , Å ³	5849.0(9)	5102(2)	2447.2(7)	6491(3)
<i>Z</i>	4	4	1	4
formula weight	1040.6	925.4	1734.6	1075.7
space group	C2/c	P1	P1	Cc
<i>t</i> , °C	22	−140	22	20
λ, Å	1.541 78	1.541 78	1.541 78	0.710 73
ρ _{calc} , g cm ^{−3}	1.182	1.205	1.177	1.101
μ, cm ^{−1}	18.86	21.03	21.63	2.07
transm coeff	0.711–1.000	0.427–1.000	0.851–1.000	0.970–1.000
<i>R</i> ^a	0.060	0.070	0.052	0.050 [0.051] ^d
<i>wR</i> ^{2b}	0.166	0.215	0.153	0.128 [0.133] ^d
GOF ^c	1.077	1.103	1.036	0.996

^a $R = \sum |\Delta F| / \sum |F_o|$ calculated on the unique observed data [$I > 2 \sigma(I)$]. ^b $wR^2 = [\sum w|\Delta F|^2 / \sum w|F_o|^2]^{1/2}$ calculated on the unique data having $I > 0$. ^c GOF = $[\sum w|\Delta F|^2 / (\text{NO} - \text{NV})]^{1/2}$. ^d Values in square brackets refer to the “inverted” structure.

(CD₂Cl₂, 298 K): δ 7.79 (m, 2H, ArH(CH₂Ph)), 7.61 (m, 2H, ArH(CH₂Ph)), 7.53 (m, 1H, ArH(CH₂Ph)), 7.25 (s, 4H, ArH), 6.89 (s, 4H, ArH), 6.85 (m, 2H, ArH(CH₂Ph)), 6.77 (m, 1H, ArH(CH₂Ph)), 6.73 (m, 2H, ArH(CH₂Ph)), 4.15 (d, *J* = 13.2 Hz, 4H, *endo*-CH₂), 3.82 (s, 6H, MeO), 3.53 (s, 2H, Zr-CH₂Ph), 3.47 (d, *J* = 13.2 Hz, 4H, *exo*-CH₂), 2.80 (brs, 2H, B-CH₂Ph), 1.30 (s, 18H, Bu^t), 0.95 (s, 18H, Bu^t). ¹H NMR (C₆D₆, 298 K): δ 7.24–6.80 (m, 14H, ArH), 6.70 (s, 4H, ArH), 3.89 (d, *J* = 12.9 Hz, 4H, *endo*-CH₂), 3.48 (s, 2H, CH₂Ph), 3.15 (d, 4H, *exo*-CH₂), overlapping with 3.14 (s, 6H, MeO), 2.97 (s, 2H, CH₂Ph), 1.34 (s, 18H, Bu^t), 0.70 (s, 18H, Bu^t). Anal. Calcd for **21**, C₇₈H₇₂BF₁₅O₄Zr: C, 64.15; H, 4.97. Found: C, 63.88; H, 4.99. Dilute C₆D₆ solutions of the product are thermally stable (3 h, 60 °C). It is unstable in CD₂Cl₂ (at room temperature, the reaction is complete in hours). It is photosensitive. It reacts with THF to give the adduct; a small amount of **21** was dissolved in THF, volatiles were removed *in vacuo*, and the residue was dissolved in CD₂Cl₂. ¹H NMR (CD₂Cl₂, 298 K): δ 7.62–6.71 (m, 18H, ArH), 4.16 (d, *J* = 12.9 Hz, 4H, *endo*-CH₂), 3.90 (m, 12H, THF), overlapping with 3.83 (s, 6H, MeO), 3.45 (d, *J* = 12.9 Hz, 4H, *exo*-CH₂), 3.03 (s, 2H, Zr-CH₂Ph), 2.80 (br s, 2H, B-CH₂Ph), 1.93 (m, 12H, THF), 1.28 (s, 18H, Bu^t), 1.08 (s, 18H, Bu^t). It does not react with THF.

Synthesis of 22. 10·(thf)₂·(C₆H₆)₂ (4.49 g, 2.39 mmol) was suspended in toluene (80 mL). A solution of PhLi (14.1 mL, 0.34 M in THF, 4.79 mmol) was added dropwise over 20 min at −70 °C. The reaction mixture was allowed to warm to room temperature under stirring, and the opalescent suspension was then refluxed over 6 h, resulting in a brown suspension. Volatiles were removed, and benzene (130 mL) was then added. The residue was extracted over 36 h to yield a white precipitate of **22**·(C₆H₆)₂, which was collected and dried *in vacuo* (2.34 g, 54%). ¹H NMR (CD₂Cl₂, 298 K): δ 7.36 (s, 12H, benzene), 7.31 (m, 4H, ArH), 7.09 (d, *J* = 2.4 Hz, 4H, ArH), 7.48 (d, *J* = 2.4 Hz, 4H, ArH), 6.92 (m, 2H, ArH), 6.86 (m, 4H, ArH), 6.80 (s, 4H, ArH), 6.55 (s, 4H, ArH), 4.73 (d, *J* = 13.0 Hz, 4H, *endo*-CH₂), 4.36 (d, *J* = 12.3 Hz, 4H, *endo*-CH₂), 3.18 (d, *J* = 12.3 Hz, 4H, *exo*-CH₂), 2.84 (s, 6H, MeO), overlapping with 2.84 (d, *J* = 13.0 Hz, 4H, *exo*-CH₂), 1.28 (s, 36H, Bu^t), 1.02 (s, 18H, Bu^t), 0.97 (s, 18H, Bu^t). Anal. Calcd for **22**·(C₆H₆)₂, C₁₁₄H₁₃₂O₈Zr₂: C, 75.54; H, 7.34. Found: C, 75.16; H, 7.51.

Synthesis of 23. A solution of Bu^tNC (0.239 g, 2.87 mmol) in toluene (34 mL) was added dropwise at −50 °C to a suspension of **22**·(C₆H₆)₂ (2.54 g, 1.40 mmol) in toluene (90 mL). The resulting yellow solution was allowed to warm to room temperature with stirring overnight. The reaction mixture was then refluxed for 12 h, volatiles were removed *in vacuo*, and hexane (30 mL) was added to the residue. The flask was kept 1 day at −24 °C, and then white **23**·C₇H₈·C₆H₁₄ solid was collected and dried *in vacuo* (0.803 g, 26%). ¹H NMR (CD₂Cl₂, 298 K): δ 7.5–6.97 (m, 18H, ArH), 4.65 (d, *J* = 12.2 Hz,

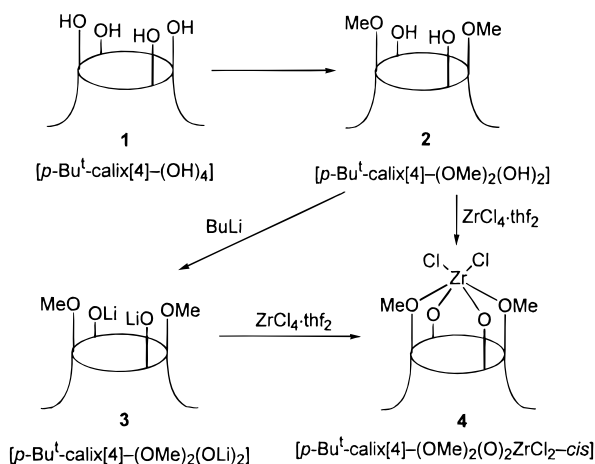
2H, *endo*-CH₂), 4.30 (d, *J* = 12.2 Hz, 2H, *endo*-CH₂), 4.19 (s, 3H, MeO), 3.30 (d, *J* = 12.2 Hz, 2H, *exo*-CH₂), 3.17 (d, *J* = 12.2 Hz, 2H, *exo*-CH₂), 2.34 (s, 3H, C₇H₈), 1.62 (s, 9H, Bu^t), 1.31 (m, 8H, CH₂-hexane), 1.23 (s, 18H, Bu^t), 1.15 (s, 9H, Bu^t), 1.14 (s, 9H, Bu^t), 0.88 (m, 6H, CH₂-hexane). ¹H NMR (C₆D₆, 298 K): δ 7.38 (d, *J* = 2.4 Hz, 2H, ArH), 7.26 (d, *J* = 2.4 Hz, 2H, ArH), 7.05 (m, 2H, ArH), 6.98 (s, 2H, ArH), 6.93 (s, 2H, ArH), overlapping with 6.92 (m, 1H, ArH), 6.74 (m, 2H, ArH), 5.16 (d, *J* = 12.0 Hz, 2H, *endo*-CH₂), 4.46 (d, *J* = 12.0 Hz, 2H, *endo*-CH₂), 3.92 (s, 3H, MeO), 3.58 (d, *J* = 12.0 Hz, 2H, *exo*-CH₂), 3.31 (d, *J* = 12.0 Hz, 2H, *exo*-CH₂), 2.10 (s, 3H, C₇H₈), 1.57 (s, 9H, Bu^t), 1.46 (s, 18H, Bu^t), 1.23 (m, 8H, hexane), 0.92 (s, 9H, Bu^t), 0.88 (m, 6H, C₆H₁₄), 0.73 (s, 9H, Bu^t). Anal. Calcd for **23**·C₇H₈·C₆H₁₄, C₆₉H₉₁NO₄Zr: C, 76.05; H, 8.42, N, 1.29. Found: C, 76.30; H, 8.46; N, 1.13. Crystals suitable for X-ray analysis were obtained from a saturated solution in *n*-hexane. The product is stable to prolonged heating (90 °C, 12 h) in C₆D₆, as judged by ¹H NMR.

X-ray Crystallography for Complexes 13, 16, 22, and 23. Crystal data and details associated with data collection are listed in Tables 1 and S2. The structures were solved by the heavy-atom method starting from a three-dimensional Patterson map.¹² Refinements were done by full-matrix least-squares first isotropically and then anisotropically for all non-H atoms except for some disordered atoms. In the last stage of refinement, the weighting scheme $w = 1/[\sigma^2(F_o^2) + (aP)^2]$ (with $P = (F_o^2 + 2F_c^2)/3$) was applied, with *a* resulting in the value of 0.0724, 0.1443, 0.1062, and 0.0922 for **13**, **16**, **22**, and **23**, respectively. All calculations were performed by using SHELX92.¹³ Except for those related to the disordered atoms and to the *n*-hexane solvent molecule in **23**, which were ignored, the hydrogen atoms for all complexes were located from difference Fourier maps and introduced in the subsequent refinements as fixed atom contributions with isotropic *U*'s fixed at 0.10 Å² for **13** and **22** and at 0.08 Å² for **16** and **23**. The hydrogen atoms associated to the benzene solvent molecules in **22** and **23** were put in geometrically calculated positions with the isotropic *U*'s fixed at 0.20 Å². In complex **13**, a Bu^t group of calixarene was affected by high thermal parameters, indicating the presence of disorder, which was solved by splitting the C30, C31, and C32 methyl carbon atoms over two positions (A and B), isotropically refined with site occupation factors of 0.7 and 0.3, respectively, applying a constraint to the C–C bond distances [1.54(1) Å]. In complex **16**, a Bu^t group of molecule A was affected by high thermal parameters, indicating the presence of disorder. The best fit was obtained by splitting the C42, C43, and C44 methyl carbon atoms over three positions (C, D, E), isotropically refined with a site occupation factor of 0.3333. In complex **22**, troubles

(12) Sheldrick, G. M. SHELX76. Program for crystal structure determination; University of Cambridge, England, 1976.

(13) Sheldrick, G. M. SHELXL92. Program for Crystal Structure Refinement; University of Göttingen, Germany, 1992.

Scheme 1



were encountered in refining the structure because of the rather high values reached by the U_{ij} parameters of all the Bu^t groups, indicating some disorder, which was solved by splitting the atoms as follows: C30, C31, and C32 over three positions ($A = 50\%$, B and $C = 25\%$); C34, C35, and C36 over two positions ($A = B = 50\%$); C38, C39, and C40 over three positions ($A = B = C = 33\%$); C42 and C43 over two positions ($A = B = 50\%$); and C44 over three positions ($A = B = C = 33\%$). During the refinement, the C–C bond distances within the Bu^t groups were constrained to $1.54(1)$ Å. In complex **23**, all four Bu^t groups of calixarene were found to be affected by disorder, which was solved by splitting all the methyl carbon atoms over two positions (A and B), isotropically refined with site occupation factors of 0.5, applying a constraint to the C–C bond distances [$1.54(1)$ Å]. See the Supporting Information for more details.

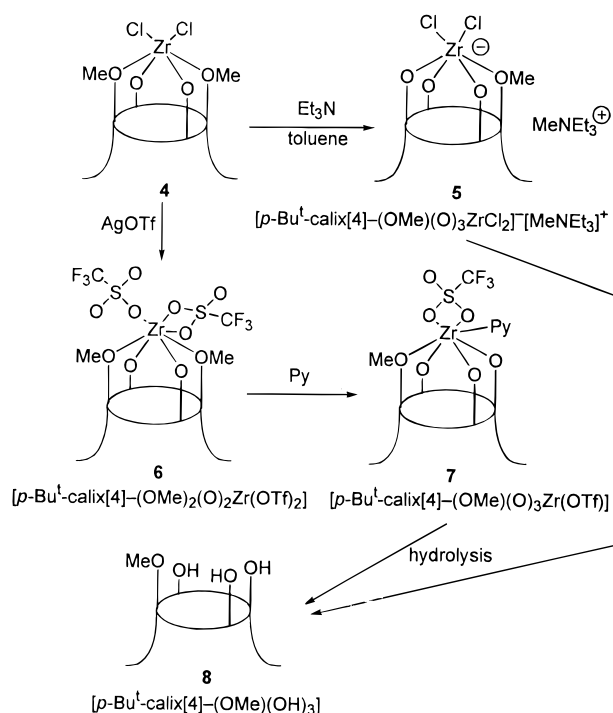
Results

The Parent Compounds. The parent compound **4**, which serves as starting material for the organometallic derivatization of zirconium calix[4]arene, has been prepared according to two procedures, which are outlined in Scheme 1.

The synthesis avoiding the use of any alkali salt is preferred in this kind of chemistry because the alkali salt very often remains complexed by the ensuing calix[4]arene moiety,¹⁴ while that passing through the intermediate **3** gave higher yields when carried out *in situ*. Complex **4** crystallizes with two molecules of benzene, one being hosted in the calix[4]arene cavity. The ^1H NMR spectrum is as expected for a cone conformation having a C_{2v} symmetry; thus, the methylene groups appear as one pair of doublets and the Bu^t as two singlets (see the Experimental Section). The proposed structure has been supported by an X-ray analysis, which is included in the Supporting Information. Before showing the organometallic functionalization which can be carried out on **4**, we should emphasize that **4** undergoes demethylation reactions in the presence of relatively strong bases (*i.e.*, NEt_3 , Py) (see Scheme 2), with the formation of the corresponding ammonium or pyridinium salts.

In the reaction with Et_3N , compound **5** was isolated, which contains the monomethoxycalix[4]arene trianion. The difficulty in separating the $\text{Et}_3\text{NMe}^+\text{Cl}^-$ salt from the Zr–calix[4]arene moiety suggests that the Cl^- is still bonded to the metal, either outside (see the picture in Scheme 2) or inside the cavity, giving rise to a *trans*-dichloro derivative. The same derivatization reaction was achieved by reacting **4** with pyridine. In both cases, the reaction of **4** with a base (Et_3N or Py), followed by hydrolysis, gave clean **8**. The Zr–Cl functionality in **4** is very reactive in metathesis reactions. The ionization of the Zr–Cl

Scheme 2



bonds was achieved in the reaction of **4** with AgOTf . This reaction has, among others, the purpose of producing a Lewis acid, where zirconium is only weakly bound to the OTf^- anion.^{15,16} The reaction is carried out in benzene, since the Lewis acidity of zirconium in **6** promotes THF polymerization. The X-ray structure of **6** (see the Supporting Information) revealed the two bonding modes shown for the OTf^- anion. The use of **6** as a Lewis acid promoter of a variety of organic reactions is currently under investigation, though **6** suffers from the limitation of undergoing demethylation in the presence of strong bases like pyridine. The base-induced demethylation of **6** to **7** has been followed by ^1H NMR spectroscopy. The hydrolysis of **7** gave, as expected, the free monomethoxycalix[4]arene (**8**).

The demethylation of **4** and **6** led us to develop an appropriate synthetic approach to the monochlorozirconium(IV) calix[4]arene, which can be an attractive parent compound for the organometallic functionalization. The synthetic procedure is shown in Scheme 3 and reported in detail in the Experimental Section, while a detailed discussion on the synthesis of **8** will be part of a forthcoming paper.¹⁷

The dimeric structure proposed for **10** in the solid state is based on the analogous structure found for the corresponding phenyl derivative (*vide infra*, complex **22**). As a matter of fact, a monomeric form can be obtained in the presence of a strongly binding ligand. The reaction of **10** with an excess of pyridine gave the monomer **11** (Scheme 3), in which the methoxy group is also displaced. A preliminary X-ray analysis shows a $\text{Zr}\cdots\text{OMe}$ distance longer than 2.75 Å in **11**.¹⁸

The Synthesis of Zr–C Bonds. The alkylation of **4** (path *b*, Scheme 4) has been performed according to conventional

(15) Gennari, C. In *Comprehensive Organic Synthesis*, Heathcock, C. H., Ed.; Pergamon: Oxford, U.K., 1991; Vol. 1. Beck, W.; Sunkel, K. *Chem. Rev.* **1988**, *88*, 1405.

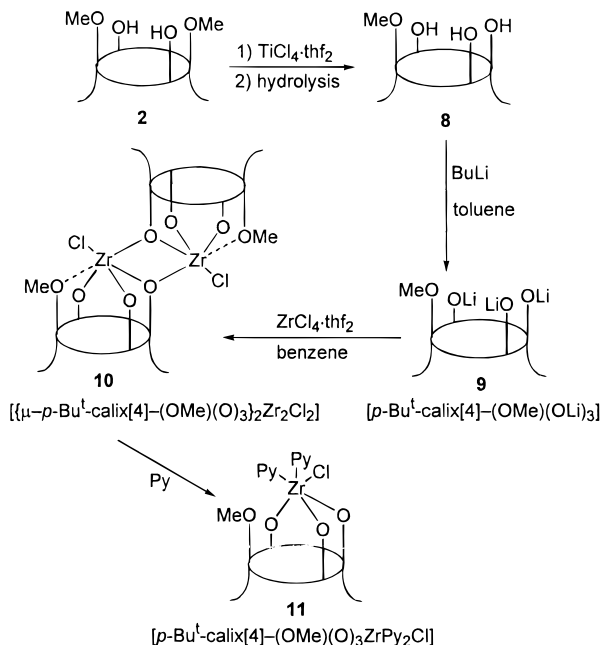
(16) Cozzi, P. G.; Floriani, C.; Chiesi-Villa, A.; Rizzoli, C. *Synlett* **1994**, 857.

(17) Zanotti-Gerosa, A.; Floriani, C., manuscript in preparation.

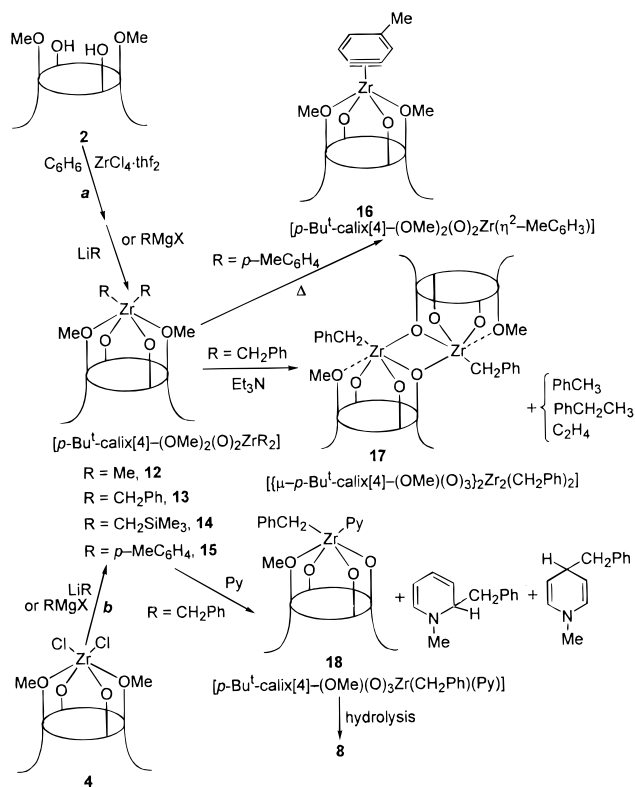
(18) Crystal data for **11**: $\text{C}_{55}\text{H}_{65}\text{N}_2\text{O}_4\text{Zr}\cdot\text{C}_5\text{H}_5\text{N}$, $M = 1458.96$, triclinic, space group $a = 16.757(3)$, $b = 19.195(3)$, and $c = 12.930(2)$ Å, $\alpha = 99.62(2)^\circ$, $\beta = 100.76(2)^\circ$, $\gamma = 82.92(2)^\circ$, $V = 4010.13(12)$ Å³, $Z = 2$, $d_{\text{calc}} = 1.2083$ g cm^{-3} , $F(000) = 1542.0$, $\mu = 18.527$ cm^{-1} , $\lambda = 1.54178$ Å.

(14) Zanotti-Gerosa, A.; Solari, E.; Giannini, L.; Floriani, C.; Chiesi-Villa, A.; Rizzoli, C. *Chem. Commun.* **1997**, 183 and references therein.

Scheme 3



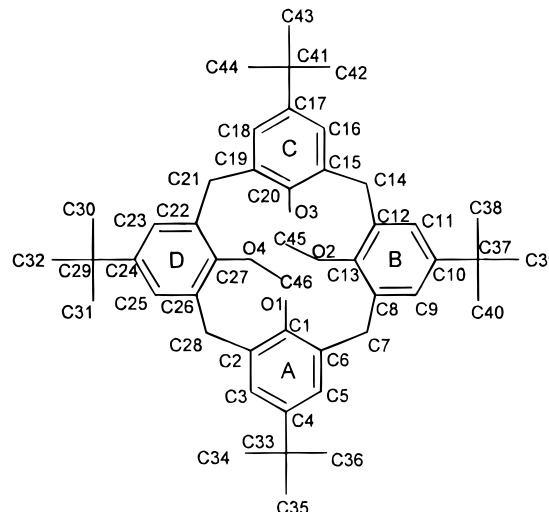
Scheme 4



procedures using lithium or Grignard reagents. The preliminary isolation of **4** is not compulsory; thus, the synthesis of the zirconium alkyl or aryl derivatives can be carried out *in situ* directly from **2** (path a, Scheme 4), using the sequence specified in the Experimental Section.

The ^1H NMR spectra of **12–15** all imply C_{2v} symmetry, as revealed by the CH_2 (one pair of doublets), Bu^t (two singlets), and MeO (one singlet) patterns. The synthesis of pure monoalkylchloro derivatives is prevented by the facile redistribution reaction between dichloro and dialkyl derivatives; for example, mixing equimolar amounts of **4** and **12** in CD_2Cl_2 gives an equilibrium mixture of **4**, **12**, and $[p\text{-Bu}^t\text{-calix[4]-(OMe)}_2(\text{O})_2\text{-Zr}(\text{Cl})(\text{Me})]$ (see the Experimental Section). All the alkyl

Chart 2



derivatives **12–14** are thermally stable up to 80°C in C_6D_6 . Further, they are not particularly light-sensitive, though the photolysis of **12** in CD_2Cl_2 gave **4**. Under strong solar light (or UV irradiation), they all undergo reaction/decomposition. The aryl derivative **15** is more thermally sensitive than the corresponding alkyl compounds **12–14**, and refluxing in benzene for 36 h gave the corresponding benzyne derivative, **16**, *via* toluene elimination.^{6f,19} The analogous α -elimination, leading to the corresponding alkylidene,²⁰ has never been observed in the case of the attempted thermal decomposition of **12–14**. The reactivity study on **12–15** should take into account the base-induced demethylation of one of the methoxy groups when they are treated with a relatively strong base. The reaction of **13** with pyridine gave the concomitant demethylation of the methoxy group and the dealkylation at the metal leading to **18** and to the organic products obtained by reacting $(\text{PhCH}_2)_2\text{-Mg}$ and *N*-methylpyridinium $\cdot\text{BPh}_4$, as revealed by NMR analysis. In the case of Et_3N , demethylation led to **17** and a mixture of toluene, ethylbenzene, and ethylene. The obtention of **17** rather than the corresponding solvated form depends on the low affinity of Et_3N for zirconium(IV). Complex **17** has also been obtained from the alkylation of **10**, as shown in Scheme 6. The key compounds **13** and **16** in Scheme 4 have been characterized by X-ray analyses.

The labeling scheme adopted for the calixarene moiety for all complexes is indicated in Chart 2. Selected bond distances and angles for complexes **13**, **16**, **22** and **23** are quoted in Tables 2 and 3. A comparison of relevant conformational parameters is reported in Table 4. The structure of complex **13**, hosting a toluene molecule in the cavity, is shown in Figure 1.

The complex molecule possesses a crystallographically imposed C_2 symmetry, the two-fold axis running through the molecular axis. The distorted octahedral coordination around zirconium is provided by the four oxygen atoms from calixarene and by the C51 and C51' methylene carbon atoms from two symmetry-related benzyl ligands ($' = -x, y, 0.5 - z$). As a

(19) (a) Buchwald, S. L.; Broene, R. D. In *Comprehensive Organometallic Chemistry II*; Abel, E. W., Stone, F. G. A., Wilkinson, G., Eds.; Pergamon: Oxford, 1995; Vol. 12, Chapter 7.4 and references therein. (b) Erker, G.; Albrecht, M.; Krüger, C.; Werner, S. *J. Am. Chem. Soc.* **1992**, *114*, 8531. (c) Buchwald, S. L.; Fischer, R. A.; Foxman, B. M. *Angew. Chem., Int. Ed. Engl.* **1990**, *29*, 771. (d) Buchwald, S. L.; Lucas, E. A.; Davis, W. M. *J. Am. Chem. Soc.* **1989**, *111*, 397. (e) Bennett, M. A.; Schwemlein, H. P. *Angew. Chem., Int. Ed. Engl.* **1989**, *28*, 1296. (f) Binger, P.; Biedebach, B.; Mynott, R.; Regitz, M. *Chem. Ber.* **1988**, *121*, 1455. (g) Buchwald, S. L.; Watson, B. T.; Huffman, J. C. *J. Am. Chem. Soc.* **1986**, *108*, 7411.

(20) Fryzuk, M. D.; Mao, S. S. H. *J. Am. Chem. Soc.* **1993**, *115*, 5336.

Table 2. Selected Bond Distances (Å) and Angles (deg) for Complexes **13** and **16**

Complex 13					
Zr1–O1	1.960(3)		C51–Zr1–C51'	83.7(2)	
Zr1–O2	2.298(5)		O2–Zr1–O2'	153.9(2)	
Zr1–C51	2.332(5)		O1–Zr1–O1'	102.4(2)	
			Zr1–O1–C1	175.9(3)	
			Zr1–O2–C13	118.2(3)	
Complex 16					
	mol A	mol B		mol A	mol B
Zr1–O1	1.985(3)	1.982(4)	C51–C52	1.386(8)	1.383(10)
Zr1–O2	2.322(3)	2.346(4)	C51–C56	1.407(7)	1.408(7)
Zr1–O3	1.955(4)	1.978(3)	C52–C53	1.399(10)	1.396(11)
Zr1–O4	2.335(4)	2.325(4)	C53–C54	1.393(7)	1.354(9)
Zr1–C51	2.172(6)	2.185(5)	C54–C55	1.402(10)	1.430(14)
Zr1–C52	2.175(7)	2.179(6)	C55–C56	1.376(10)	1.378(11)
			C55–C57	1.495(9)	1.489(10)
O2–Zr1–O4	154.1(2)	1.531(2)	Zr1–O1–C1	156.5(3)	161.8(4)
O1–Zr1–O3	127.9(2)	126.7(2)	Zr1–O2–C13	114.7(4)	113.6(3)
C51–Zr1–C52	37.2(2)	37.0(2)	Zr1–O3–C20	167.3(4)	163.0(4)
			Zr1–O4–C27	114.5(3)	116.0(3)

Table 3. Selected Bond Distances (Å) and Angles (deg) for Complexes **22** and **23**

Complex 22			
Zr1–O1	1.952(2)	Zr1–O4	2.197(3)
Zr1–O2	2.662(3)	Zr1–O4'	2.185(2)
Zr1–O3	1.929(2)	Zr1–C51	2.282(6)
O4–Zr1–O4'	64.1(1)	Zr1–O1–C1	162.4(2)
O1–Zr1–O3	122.3(1)	Zr1–O2–C13	112.8(2)
O3–Zr1–O4	89.0(1)	Zr1–O3–C20	161.2(2)
O2–Zr1–O4	151.0(1)	Zr1–O4–Zr1'	115.9(1)
Zr1–O4–C27	111.6(2)	Zr1'–O4–C27	132.5(2)
Complex 23			
Zr1–O1	1.954(3)	Zr1–C51	2.260(3)
Zr1–O2	2.403(3)	N1–C51	1.269(4)
Zr1–O3	1.966(3)	N1–C58	1.482(4)
Zr1–O4	2.037(2)	C51–C52	1.462(4)
Zr1–N1	2.180(3)		
N1–Zr1–C51	33.1(1)	Zr1–O4–C27	122.8(2)
O2–Zr1–O4	156.4(1)	Zr1–N1–C58	147.1(3)
O1–Zr1–O3	129.6(1)	Zr1–N1–C51	76.9(2)
Zr1–O1–C1	154.7(3)	C51–N1–C58	136.0(4)
Zr1–O2–C13	118.4(2)	Zr1–C51–N1	70.0(2)
Zr1–O3–C20	155.0(3)		

consequence of the six-coordination of the metal, the planarity of the O₄ core is completely removed,^{5d,14} the best coordination plane being defined by the O1, O2, O2', and C51 atoms. As is usually observed for six-coordinated calixarene metal complexes, the macrocycle ligand assumes an elliptical cross section conformation, with the A and C rings pushed outward from and the B and D rings inward to the cavity, as indicated by the dihedral angles they form with the “reference plane” (Table 4). The elliptical section of the cavity can be indicated by the values of the distances between opposite *para*-carbon atoms: C4···C4', 9.811(7) Å; C10···C10', 7.081(8) Å. The O₄ core shows tetrahedral distortions ranging from –0.355(4) to 0.355(4) Å, the metal being displaced by 0.873(1) Å from the mean plane. The C52–C57 aromatic ring of the benzyl ligand forms a dihedral angle of 57.0(4)° with the O₄ mean plane. The Zr–O1 bond distance [1.960(3) Å] is in agreement with those in zirconium phenoxo complexes^{10b,j} and is consistent with some double bond character supported by the approximate linearity of the Zr–O1–C1 bond angle (Table 2). The Zr–O2 bond distance involving the methoxy group is remarkably longer [2.298(5) Å]. The Zr–C51 bond distance [2.332(5) Å] has the value expected for a Zr–C(sp³) carbon.⁷ The guest toluene

molecule enters the cavity with the aromatic ring perpendicular to the A ring [dihedral angle 92.2(5)°] and nearly parallel to the B ring [dihedral angle 19.2(5)°]. The minimum Zr···C(toluene) distance [Zr···C66, 5.391(12) Å] rules out any possible interaction involving the metal atom. As a consequence of the asymmetry of the cavity, the toluene axis is tilted with respect to the molecular axis, giving rise to a statistical distribution of the solvent molecule. In spite of the disorder, host–guest interactions seem to take place involving the C35 methyl group associated to the B ring and the aromatic ring of toluene, as suggested by the following distances: C35···C61, 3.61(2) Å; C61···H351, 2.54 Å; C35···C62, 3.70(2) Å; C62···H351, 2.62 Å; C35···C62', 3.86(2) Å; C62'···H351, 2.78 Å.

The structure of **16**, which contains a toluene of crystallization in the 1:0.75 Zr–toluene ratio, is reported in Figure 2. In the unit cell, there are two crystallographically independent molecules (A and B) showing a close geometry. The values referring to molecule B will be, hereafter, given in square brackets.

The calixarene macrocycle assumes an elliptical cross section conformation, probably as a consequence of the orientation of the η²-bonded ligand, which forces the B and D rings to bend toward the cavity of calixarene. With respect to complex **13**, the conformation mainly differs in the orientation of aromatic rings which are closer to be mutually perpendicular (A and C) and parallel (B and D) to each other (Table 4). This results in a more pronounced elliptical nature of the cavity and thus prevents the inclusion of toluene, which is present in the structure as a crystallization solvent and not as a guest. The trend in the Zr–O bond distances (Table 2) is similar to that observed in **13**. The η²-bonded benzyne shows a symmetric bonding mode to the metal, the Zr–C51 and Zr–C52 bond distances being very close. Their mean value [2.173(5) Å] is remarkably shorter than those found for Zr–C σ bonds (see complexes **13** and **22**). The C–C bond distances within the benzyne ring are very close without alternation of short and long bond lengths. Such a trend of structural data is quite close to that observed in [Cp₂Zr(η⁶-C₆H₄)(PMe₃)].^{19g} The plane of the η²-bonded atoms (Zr, C51, C52) is nearly perpendicular to the mean plane through the O₄ core {dihedral angle 84.2(2) [89.2(2)]°}, and the direction of the C51–C52 bond is parallel to the O2···O4 line {2.7(3) [3.6(3)]°}. The O₄ core has some tetrahedral distortion (displacements ranging from –0.172(4)

Table 4. Comparison of Relevant Conformational Parameters within Calixarene for Complexes **13**, **16**, **22** and **23**

	13	16	22	23	
	(a) Dihedral Angles (deg) between Planar Moieties ^b				
E \wedge A	144.8(2)	132.7(1)	[133.9(2)]	134.4(1)	132.6(1)
E \wedge B	109.6(2)	98.4(2)	[96.7(2)]	100.2(1)	110.7(1)
E \wedge C	144.8(2)	136.8(1)	[135.7(1)]	134.5(1)	132.0(1)
E \wedge D	109.6(2)	97.4(2)	[100.7(2)]	93.8(1)	116.5(1)
A \wedge C	109.7(2)	90.5(2)	[90.4(2)]	91.0(2)	95.4(1)
B \wedge D	140.8(2)	164.2(2)	[162.5(2)]	166.0(2)	132.9(1)
	(b) Contact Distances (Å) between <i>para</i> -Carbon Atoms of Opposite Aromatic Rings ^c				
C4...C17	9.811(7)	9.412(6)	[9.431(9)]	9.290(6)	9.101(8)
C10...C24	7.081(8)	5.884(8)	[5.948(10)]	5.766(8)	7.462(5)

^a Values in square brackets refer to molecule **B**. ^b **E** (reference plane) refers to the least-squares mean plane defined by the C7, C14, C21, C28 bridging methylenic carbons. **A**, **B**, **C**, and **D** refer to the least-squares mean planes defined by the aromatic rings bonded to O1, O2, O3, and O4, respectively. O3, O4, C21, and C28 should be read O1', O2', C7', and C14', respectively, in complex **13** ($\ell' = -x, y, 0.5 - z$). ^c In complex **13**, C17 and C24 should be read C4' and C10' respectively ($\ell' = -x, y, 0.5 - z$).

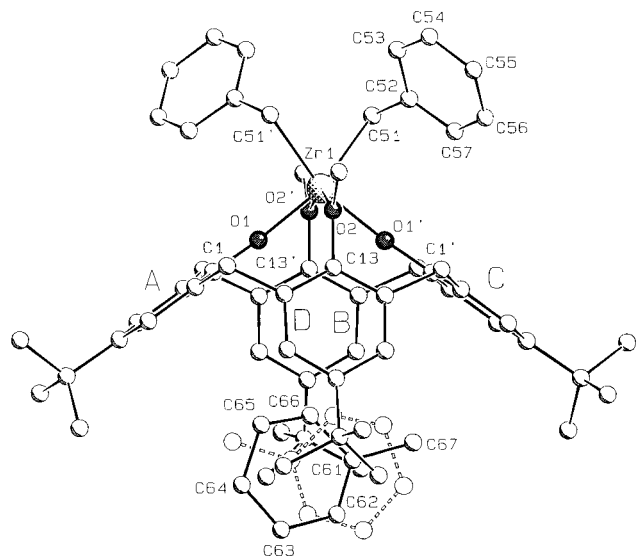


Figure 1. SCHAKAL view of complex **13**, showing the disorder affecting the guest toluene molecule. Disorder involving the Bu^t groups has been omitted for clarity. Prime denotes a transformation of $-x, y, 0.5 - z$.

$[-0.175(4)]$ to $0.173(4)$ [$0.173(4)$ Å], zirconium protruding by $0.693(2)$ [$0.715(2)$ Å] from the mean plane. The most significant difference between molecules **A** and **B** consists in the orientation of the plane through the C51–C57 atoms with respect to the O4 mean plane $\{75.7(2)$ [$89.9(2)^\circ$].

Compounds **12**–**15** are particularly appropriate precursors for the corresponding monoalkyl cationic species, which, especially in the case of $[\text{Cp}_2\text{Zr}]$ chemistry,²¹ are still receiving a lot of attention as polymerization catalysts. The generation of cationic species has been achieved *via* two major routes: (i) the one-electron oxidation using $[\text{Cp}_2\text{Fe}]^+\text{BPh}_4^-$ to generate **19** in toluene or **20** in a coordinating solvent like THF^{8c,21} and (ii) the reaction with a Lewis acid, like $[\text{B}(\text{C}_6\text{F}_5)_3]$, to give **21** (Scheme 5).^{21,22}

We should mention that **19** undergoes a thermally induced (90°C , 1 h, C_6D_6) disproportionation reaction with simultaneous arylation of zirconium by BPh_4^- , thus forming **13** and **22**. The

(21) Guram, A. S.; Jordan, R. F. In *Comprehensive Organometallic Chemistry II*; Abel, E. W., Stone, F. G. A., Wilkinson, G., Eds.; Pergamon: Oxford, 1995; Vol. 4, Chapter 12. Yang, X.; Stern, C. L.; Marks, T. J. *J. Am. Chem. Soc.* **1994**, *116*, 10015. Guerra, G.; Cavallo, L.; Moscardi, G.; Vacatello, M.; Corradini, P. *J. Am. Chem. Soc.* **1994**, *116*, 2988. Erker, G.; Aulbach, M.; Knickmeier, M.; Wingbermhühle, D.; Krüger, C.; Nolte, M.; Werner, S. *J. Am. Chem. Soc.* **1993**, *115*, 4590. Coates, G. W.; Waymouth, R. M. *J. Am. Chem. Soc.* **1993**, *115*, 91. Jordan, R. F. *Adv. Organomet. Chem.* **1991**, *32*, 325.

(22) Yang, X.; Stern, C. L.; Marks, T. J. *J. Am. Chem. Soc.* **1991**, *113*, 3623.

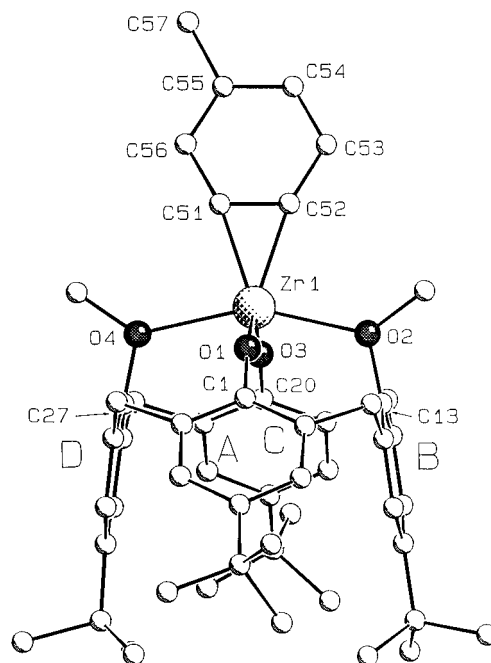


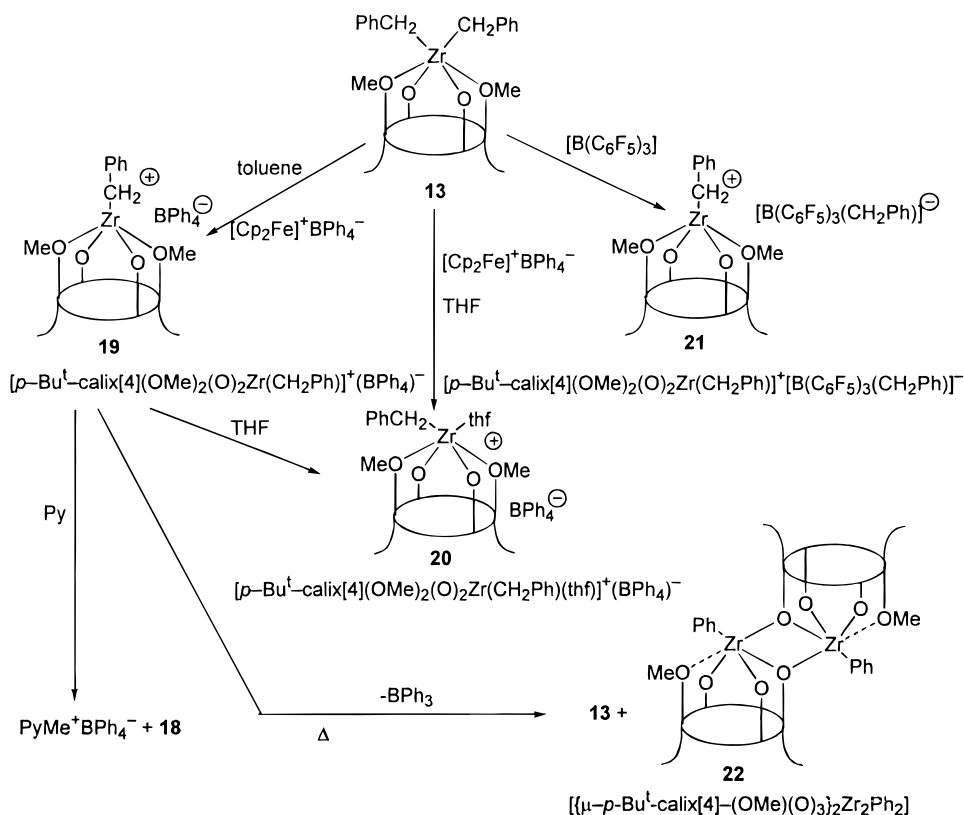
Figure 2. SCHAKAL view of molecule **A** of complex **16**. Disorder has been omitted for clarity.

cationic species **19** and **21** have C_{2v} symmetry, as revealed by the ^1H NMR spectrum. The Lewis acid activity of such cationic species is, somehow, not easily defined. Complex **19** reacts with THF, causing its partial polymerization, as is the case for **20**, which can be isolated free of polymeric THF only after recrystallization. The same behavior has been observed for **21**, like the photolability and the degradation in the presence of halogenated solvents, *i.e.*, CH_2Cl_2 . Both **19** and **21** did not show, however, any activity toward olefin polymerization. We believe that, in such compounds, the two methoxy groups sterically overprotect the metal center. The reaction of **19** with pyridine emphasizes the action of a strong base in the demethylation of one of the methoxy groups. The pyridine functions as the acceptor of the methyl cation and thus forms **18** and $\text{PyMe}^+\text{BPh}_4^-$.

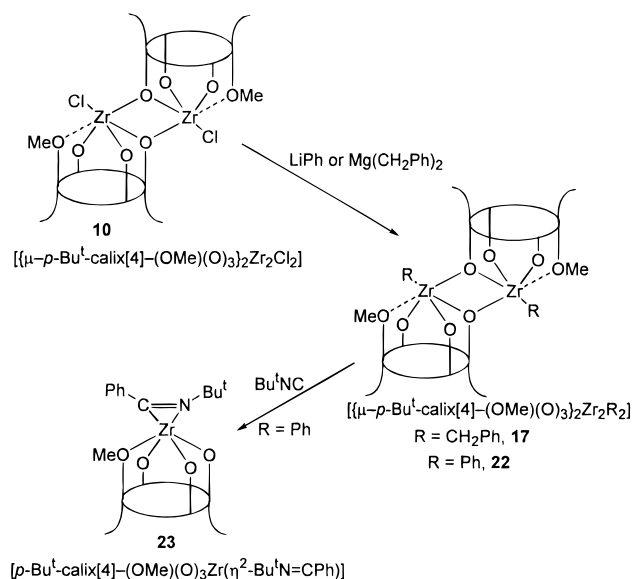
Under basic conditions, the zirconium assists the demethylation of one of the methoxy groups, especially when it is particularly acidic. In this context, we have searched for a better synthetic approach to the organometallic derivatives of the monomethoxycalix[4]arene–zirconium fragment (Scheme 6).

The reaction of **10** with LiPh gave the phenyl derivative **22**, which behaves as expected in the insertion reaction with Bu^iNC , *i.e.*, leading to an η^2 -iminoacyl, **23**.²³ The reaction causes the cleavage of the dimer into two monomeric units and

Scheme 5



Scheme 6



the methoxy group to bind zirconium. For this class of compounds, the structures of **22** and **23** will illustrate the most interesting peculiarities, including the role of the methoxy group as a spectator donor atom.

The structure of **22** consists of centrosymmetric dimers and benzene molecules of crystallization in the molar ratio 1:1 (Figure 3).

The calixarene macrocycle assumes an elliptical conformation similar to that observed in **16** (Table 4). Accordingly, the benzene solvent molecules of crystallization are not included as guests in the macrocycle. The O₄ core is tetrahedrally distorted [displacements ranging from $-0.158(2)$ to $0.146(2)$

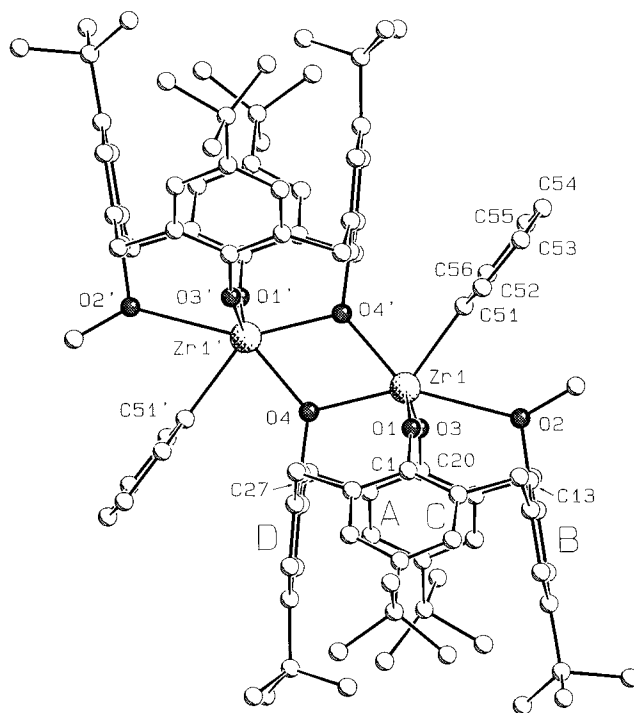


Figure 3. SCHAKAL view of complex **22**. Disorder has been omitted for clarity. Prime denotes a transformation of $-x, -y, -z$.

Å], zirconium protruding by $0.753(1)$ Å from the mean plane. The C51–C56 aromatic ring is oriented to form a dihedral angle of $54.1(2)^\circ$ with the O₄ mean plane. The Zr–O1 and Zr–O3 bond distances compare with the corresponding ones observed in **13** and **16**, while the Zr–O4 bond distances [mean value $2.191(3)$ Å] are significantly longer as a consequence of the bridging role of the O₄ oxygen atom. The Zr–O2 distance [$2.662(3)$ Å] involving the methoxy group shows a remarkable

(23) Durfee, L. D.; Rothwell, I. P. *Chem. Rev.* **1988**, *88*, 1059 and references therein.

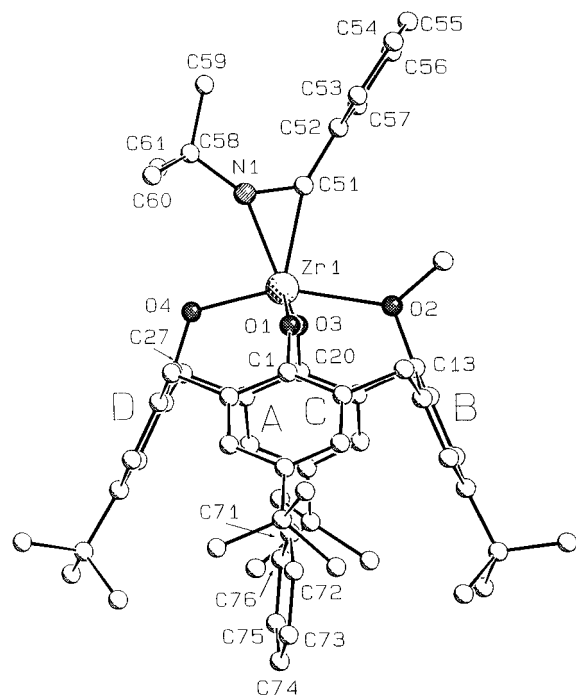


Figure 4. SCHAKAL view of complex **23**. Disorder has been omitted for clarity.

lengthening with respect to the corresponding distances in **13** and **16**, probably reflecting intraligand interactions. In particular, the H451 hydrogen atom of the C45 methoxy group points toward the C51–C56 phenyl ring at a distance of 2.54 Å from its centroid, suggesting a CH₃/π interaction.²⁴ The Zr–C bond distance [2.282(6) Å] (Table 3) is significantly shorter than that observed in **13** but is in the usual range reported for σ Zr–C(sp²) bonds.⁷

The structure of **23** contains a guest benzene molecule and an *n*-hexane solvent molecule of crystallization in the molar ratio of 1:1:1 (Figure 4). The η²-bonded N,C fragment shows a slightly asymmetric bonding mode to the metal, the Zr–N1 and Zr–C51 bond distances being 2.180(3) and 2.260(3) Å, respectively, as expected for [Zr(η²-iminoacyl)] derivatives.²³ The N1–C51 bond distance [1.269(4) Å] is consistent with a double bond character.

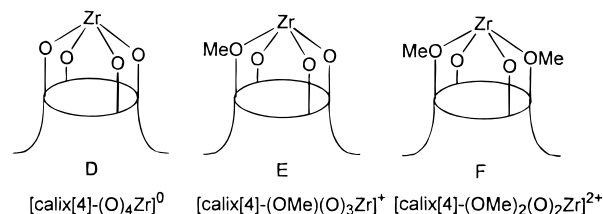
The calixarene macrocycle assumes an elliptical cross section conformation similar to that observed in complex **13**, allowing the inclusion of a benzene molecule which enters the cavity orienting its C71⋯C74 molecular axis nearly parallel to the calixarene axis, as indicated by the dihedral angle of 9.9(2)° between the C71⋯C74 line and the normal to the O₄ core and by the value of the Zr⋯C71⋯C74 angle [170.8(6)°]. Disorder affecting the Bu^t groups of calixarene prevents any sound discussion on possible host–guest interactions. The O₄ core is tetrahedrally distorted [displacements ranging from –0.259(3) to 0.154(3) Å], zirconium protruding by 0.601(1) Å from the mean plane. The plane of the η²-bonded atoms (Zr, N1, C51) is perpendicular to the O₄ mean plane [dihedral angle 91.9(2)°]. The Zr–O1 and Zr–O3 bond distances (Table 3) are close to those observed in the previous complexes, while the Zr–O4 bond distance is significantly longer.

Discussion

The results mentioned in the previous section show the variety of the Zr–C bonds we can build up over a calix[4]arene oxo surface, *i.e.*, Zr–C σ functionalities in [ZrR₂], [ZrR], and [ZrR]⁺,

(24) Andreetti, G. D.; Ugozzoli, F. In ref 4b, pp 88–122.

Chart 3



and π functionalities in [Zr-aryne]. The O₄ macrocycle is a unique chemical environment for such Zr–C fragments, because of a number of peculiarities:

(i) The topology of the O₄–Zr moiety is approximately square-pyramidal, with the metal out of the “O₄” plane.

(ii) The metal orbitals available for binding functionalities or assisting their transformations are located on the free face of the [ZrO₄] hemisandwich (*vide infra*).

(iii) The partial methylation of the phenoxo groups not only provides a variable range of charges for an O₄ set but allows one to tune the ratio between strong σ,π donor (the phenoxo) and weak σ donor oxygens (the methoxy).

(iv) The competition for the same orbitals by the O₄ set and the organometallic functionalities would be an important factor for their reactivity.

For a better understanding of the basic chemical behavior of the [ZrO₄]ⁿ⁺ [*n* = 0, 1, 2] core in binding and assisting the chemistry of organometallic functionalities, we undertook extended Hückel calculations²⁵ on the fragments in Chart 3 with the aim of studying their frontier orbitals and comparing them with those of other well-known organometallic fragments, such as [Cp₂Zr]²⁺²⁶ and [Zr(tmtaa)]²⁺²⁷. Further, we wished to rationalize the conversion of F into E (see reactions in Schemes 2, 4, and 5) in a variety of reactions with nucleophiles.

The ligands have been slightly modified by replacing the Bu^t groups and the methylene bridges by hydrogens and symmetrizing to C_{4v}, C_s, and C_{2v} geometries. The simplified models retain the main features of the whole ligand; in particular, the geometrical constraints on the O₄ set of donor atoms have been maintained by fixing the geometry of the four phenoxo groups to the experimental values observed for the mono- or the dichloro derivatives.

The lowest vacant orbitals of these fragments are depicted in Figure 5. For all such zirconium(IV) species with a d⁰ electron count, we found four low-lying empty metal-based orbitals. The d_{x²-y²}, pointing more closely toward the oxygen ligands, is pushed higher in energy, while the remaining four d orbitals are found within 1 eV. For the [calix[4]-(O)₄Zr] fragment, the LUMO is 1a₁ (d_{z²}), with a doubly degenerate 1e (d_{xz}, d_{yz}) *ca.* 0.5 eV above. Due to a slightly stronger overlap with the ligands, the 1b₂ (d_{xy}) orbital lies still 0.5 eV higher in energy. In the [calix[4]-(OMe)₂(O)₂Zr]²⁺ fragment, due to the reduced interaction with the methylated phenoxo ligands in the *xz* plane, the (d_{xz}, d_{yz}) set splits by *ca.* 1 eV into the 1b₁ (d_{xz}), which becomes the LUMO, although it is almost degenerate with the 1a₁ (d_{z²}) and the 1b₂ (d_{yz}), which is pushed higher than the 1a₂ (d_{xy}). The frontier orbitals of [calix[4]-(OMe)(O)₃Zr]⁺ are similar to those of the latter fragment. However, because of the lower molecular symmetry (C_s), the two lowest orbitals, of d_{z²} and d_{xz} character have the same a' symmetry and mix strongly, giving rise to two hybridized 1a' and 2a' orbitals, G

(25) (a) Hoffmann, R.; Lipscomb, W. N. *J. Chem. Phys.* **1962**, *36*, 2179.

(b) Hoffmann, R. *J. Chem. Phys.* **1963**, *39*, 1397.

(26) Tatsumi, K.; Nakamura, A.; Hoffmann, P.; Stauffert, P.; Hoffmann, R. *J. Am. Chem. Soc.* **1985**, *107*, 4440.

(27) Giannini, L.; Solari, E.; De Angelis, S.; Ward, T. R.; Floriani, C.; Chiesi-Villa, A.; Rizzoli, C. *J. Am. Chem. Soc.* **1995**, *117*, 5801.

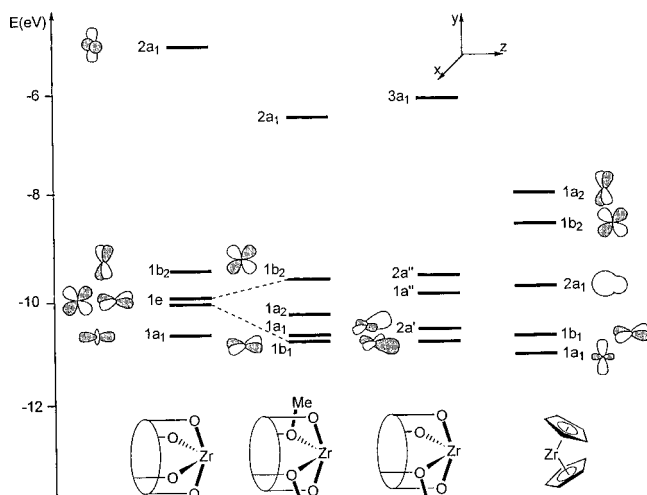
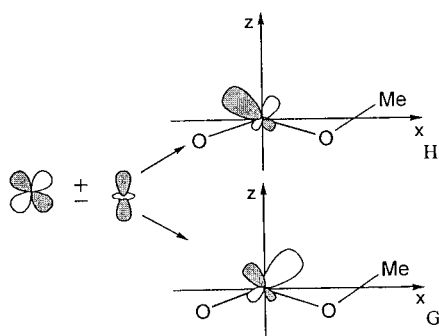


Figure 5. Frontier orbital energies for $[\text{calix}[4]\text{-(O)}_4\text{Zr}]^0$, $[\text{calix}[4]\text{-(OMe)}(\text{O})_3\text{Zr}]^+$, $[\text{calix}[4]\text{-(OMe)}_2(\text{O})_2\text{Zr}]^{2+}$, and $[\text{Cp}_2\text{Zr}]^{2+}$.

Scheme 7



and H, lying in the xz plane and tilted, respectively, toward the (O-Me) and (O) directions (see Scheme 7).

On the right of Figure 5, we report, for comparison, the well-known picture of the three low-lying empty orbitals of $[\text{Cp}_2\text{Zr}]^{2+}$ ($1a_1$, $1b_1$, and $2a_1$).²⁶ The main difference between the calix[4]arene-based fragments and $[\text{Cp}_2\text{Zr}]^{2+}$ is that, while the latter has only three low-lying empty orbitals available for bonding with additional ligands, all the three former fragments have four, and this has important consequences on their chemical behavior. Indeed, these four low-lying d orbitals can accommodate up to eight electrons, at variance with $[\text{Cp}_2\text{Zr}]^{2+}$, which can accommodate up to a maximum of six electrons without violating the EAN rule. Moreover, while in $[\text{Cp}_2\text{Zr}]^{2+}$ all the three low-lying frontier orbitals lie in the symmetry plane bisecting the Cp–Zr–Cp angle, in the calix[4]arene-based fragments only two out of the four lowest-lying orbitals are coplanar.

Most of the structures discussed in this paper can be easily rationalized on the basis of the frontier orbitals of the above fragments. Let us first consider the behavior of the fragment F. With two σ -bonding ligands, like in **4** and **12**, the metal achieves hexacoordination, with the two X^- ligands lying in the $\text{Zr}(\text{O})_2$ plane (yz). Only two of the low-lying d orbitals are used, notably $1a_1$ and $1b_2$ (d_{yz}), which interact, respectively, with the in-phase and out-of-phase combinations of the two σ -orbitals of the X^- groups, leaving as LUMO the $1b_1$ (d_{xz}) orbital. Note that the out-of-phase combination of the two σ -orbitals could, in principle, interact with the low-lying $1b_1$ (d_{xz}) orbital, leading to a different structure with the two X^- alkyl groups lying in the xz plane. Moreover, recalling that the energy of $1b_1$ is lower than that of $1b_2$ suggests that this latter structure might be of lower energy. This is, in fact, not true, as confirmed by explicit

calculations on **12** which give the latter hypothetical structure *ca.* 0.5 eV higher than that actually observed, probably because of a better overlap between the X^- σ orbitals and $1b_2$ (d_{yz}) or of steric interactions with the methyl groups in the xz plane.

A major difference between **4** and **12–15** was observed in the expected behavior as Lewis acids, and this has been substantiated by analysis of the frontier orbital energies and of the charge at the metal in **4** and **12** and by a comparison of their reactions with bases or nucleophiles. This reactivity is very important because it is responsible for the conversion of the organometallic derivatives based on fragment F into those of fragment E, as reported in Schemes 2, 4, and 5. Such a reaction can be explained as a Lewis acid-assisted cleavage of the ether bond, helped by an incoming nucleophile.²⁸ The peculiarity in the present case consists in the fact that the reaction is concerted due to the template effect of the metal. The base, Et_3N or pyridine, removes the methyl group from a methoxy residue as a carbocation (see the reaction of **19** with Py in Scheme 5, and of **4** with Et_3N in Scheme 2), and then a further reaction can occur between a nucleophile sitting on the metal and the CH_3^+ bonded to the base, as shown in the reaction of **13** with Py and Et_3N (Scheme 4). In the case of pyridine, the formation of benzyl-*N*-methyl-dihydropyridines can be explained by the nucleophilic attack of a benzyl carbanion from the metal to the methylpyridinium cation.²⁹ The demethylation of one of the methoxy groups has not only mechanistic but also has synthetic relevance, since the reaction can be used for obtaining a variety of organometallic derivatives, including the starting material of the skeleton E, from the corresponding derivatives of the skeleton F. We should mention at this stage that the synthesis of **2** is much easier than that of **8**. The conversion of the derivatives of skeleton F to those of skeleton E can be accompanied by a dimerization (see structures of **17** and **22**). Due to the relevance and generality of the reaction of bases (nucleophiles) with **4** and all its organometallic derivatives, we have been engaged in the theoretical analysis of the reaction of NH_3 (mimicking bases and nucleophiles) with **4** and **12**, which represent the limits, in terms of electronic properties, in the $[\text{calix}[4]\text{-(OMe)}_2(\text{O})_2\text{ZrX}_2]$ class of compounds.

An analysis of the frontier orbitals and of the Mulliken charges of **4** and **12** shows that, in both cases, the LUMO orbitals are essentially metal-localized and that the zirconium atom bears the highest positive charge. Therefore, we expect the metal to be the most electrophilic center in these compounds and to undergo direct attack by the base. The spatial extension of the $1b_1$ (d_{xz}) LUMO suggests that the favorable approach of the NH_3 nucleophilic species occurs along a line in the xz plane, forming an angle of approximately 45° with the z -axis. We first simulated the initial stages of the NH_3 attack by performing extended Hückel calculations on the $[\text{calix}[4]\text{-(OMe)}_2(\text{O})_2\text{ZrX}_2] \cdots \text{NH}_3$ system ($X = \text{Cl}, \text{Me}$) with (NH_3) -to-metal distances (L) ranging from 5.0 to 2.5 Å, along the expected most favorable line. At each point along the attack pathway, we relaxed the $X\text{--Zr--X}$ angle, the dihedral angle between the $\text{Zr}(\text{X})_2$ and $\text{Zr}(\text{O})_2$ planes, and also the angular position of NH_3 . The two total energy profiles are reported in Figure 6 and show that the attack is, by far, energetically more favorable for the bis-methyl than for the bis-chloro complex. For the bis-methyl complex, a small activation barrier of *ca.* 0.4 eV is observed at 3 Å but is not followed by a significant stabilization at shorter distances, therefore making the formation of a stable metal-bound intermediate questionable. A dramatically different situation is found for the bis-chloro complex, for which the energy profile

(28) March, J. *Advanced Organic Chemistry*, 4th ed., Wiley: New York, 1992; p 433.

(29) Eisner, U.; Kuthani, J. *Chem. Rev.* **1972**, *72*, 1.

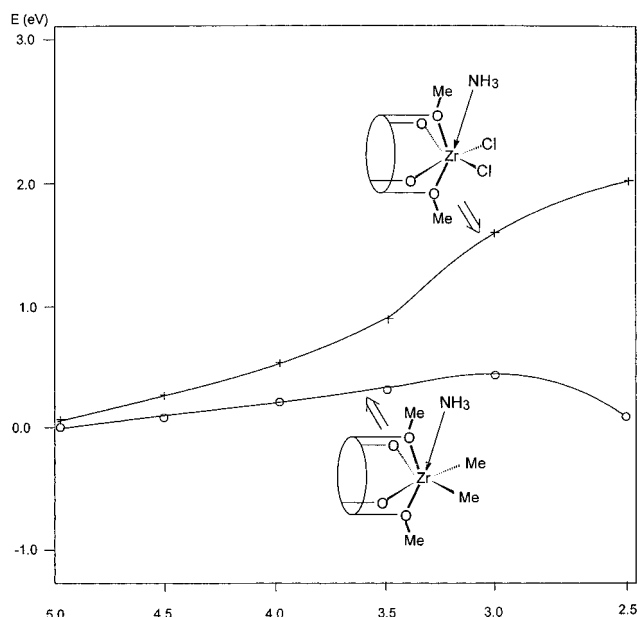
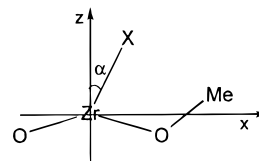


Figure 6. Total energy profile for the favored NH_3 approach toward $[\text{calix}[4]\text{-(OMe)}_2\text{(O)}_2\text{ZrMe}_2]$ and $[\text{calix}[4]\text{-(OMe)}_2\text{(O)}_2\text{ZrCl}_2]$.

continuously increases on decreasing L , reaching a difference of almost 2 eV at the lowest considered distance of 2.5 Å. This implies that the bis-chloro complex is less electrophilic than the bis-methyl analogue, in agreement with the higher energy of the LUMO orbital (-9.5 vs -10.5 eV) and the lower charge on zirconium ($+0.9$ vs $+1.1$). This suggests that, in the bis-chloro compound, the base will not attack the metal but instead removes the Me^+ group. $[\text{ZrR}_2]$ compounds are much less reactive because the preferential attack of the nucleophile to the metal center lowers its Lewis acidity and, hence, its interaction with the OMe groups. As a consequence, their tendency to be attacked by a second molecule of nucleophile is reduced.

We have subsequently considered the monomethylated calix[4]arene complexes, the simplest examples being those in which the zirconium binds only one σ ligand like Cl or Me. The most symmetrical structure for such a $[\text{calix}[4]\text{-(OMe)}(\text{O})_3\text{ZrX}]$ molecule is that in which the X^- ligand is located on the z -axis. However, on the basis of the frontier orbital analysis of $[\text{calix}[4]\text{-(OMe)}(\text{O})_3\text{Zr}]^+$ (Scheme 7) we expect the most stable structure to be slightly tilted toward the OMe group in the xz plane, to maximize the overlap of the σ orbital on the X^- ligand with the lowest vacant metal orbital, $1a'$. We have, therefore, performed a calculation on the $[\text{calix}[4]\text{-(OMe)}(\text{O})_3\text{ZrX}]$ complexes [$\text{X} = \text{Cl}, \text{R}$], varying the X-Zr-z angle α (Chart 4). However, the total energy as a function of the angle α is almost flat in a wide range around the z -axis ($\pm 30^\circ$), with a minimum for X essentially on the z -axis. This is probably due to the small energy difference between $1a'$ and $2a'$ (0.2 eV), which could be compensated by a better overlap of the σ orbital of X^- with $2a'$, which is better directed away from the $(\text{O})(\text{OMe})$

Chart 4



core. It is worth noting that the $[\text{calix}[4]\text{-(OMe)}(\text{O})_3\text{ZrX}]$ complexes still have a low-lying LUMO in the xz plane (corresponding to a suitable mixing of the $1a'$ and $2a'$ orbitals of the metal fragment) and have, therefore, a strong tendency to bind a Lewis base, giving an adduct in which the X group is tilted toward the methoxy group. This is supported by the structure of **22** (see Figure 4) in which the donating electron pair comes from the phenoxy group of an adjacent $[\text{calix}[4]\text{-(OMe)}(\text{O})_3\text{ZrX}]$ molecule, thus leading to a dimeric species.

Conclusions

This is the first series of papers on the use of an O_4 set of donor atoms, issued from a calix[4]arene cone conformation, as an oxo matrix for developing the organometallic chemistry of a transition metal. The O_4 oxo surface can be tuned in its charge and, by consequence, in its bonding mode to the metal using a partial methylation of the oxygen donor atoms from the calix[4]arene. The $[\text{calix}[4]\text{-(OMe)}_2(\text{O})_2\text{Zr}]^{2+}$ and $[\text{calix}[4]\text{-(OMe)}(\text{O})_3\text{Zr}]^+$ fragments served to model organometallic functionalities bonded to a polyoxo surface, like in catalysis,³⁰ and led to the discovery of novel reactivities and bonding modes of a variety of organic groups bonded to the metal in such an unusual O_4 coordination environment. Extended Hückel calculations on the above fragments allowed a comparison of their frontier orbitals with those of the $[\text{Cp}_2\text{Zr}]^{2+}$ fragment. In addition, using the same approach, we modeled the reaction of $[\text{calix}[4]\text{-(OMe)}_2(\text{O})_2\text{ZrX}_2]$ [$\text{X} = \text{Cl}, \text{R}$] with bases, a quite general and synthetically useful reaction allowing the conversion of two coordination environments for the same organometallic functionality.

Acknowledgment. We thank the "Fonds National Suisse de la Recherche Scientifique" (Grant No. 20-46'590.96), Ciba-Geigy S.A. (Basel), and Fondation Herbette (N.R.) for financial support.

Supporting Information Available: X-ray crystallography, ORTEP or SCHAKAL drawings, tables giving crystal data and details of the structure determination, fractional atomic coordinates, anisotropic and isotropic thermal parameters, bond lengths, and bond angles for **4**, **6**, **13**, **16**, **22**, and **23** (56 pages). See any current masthead page for ordering and Internet access instructions.

JA970821C

(30) (a) Corker, J.; Lefebvre, F.; Lecuyer, C.; Dufaud, V.; Quignard, F.; Choplin, A.; Evans, J.; Basset, J.-M. *Science* **1996**, *271*, 966. (b) Niccolai, G. P.; Basset, J.-M. *Appl. Catal., A* **1996**, *146*, 145. (c) Vidal, V.; Theolier, A.; Thivolle-Cazat, J.; Basset, J.-M.; Corker, J. *J. Am. Chem. Soc.* **1996**, *118*, 4595.